



ADDIS ABABA UNIVERSITY
ADDIS ABABA INSTITUTE OF TECHNOLOGY
SCHOOL OF MECHANICAL AND INDUSTRIAL ENGINEERING
SCHOOL OF GRADUATE STUDIES

Automobile Bumper Beam Analysis to Improve Energy Absorption

Habtamu Molla

A Thesis Submitted to the Graduate School of Addis Ababa University

In Partial Fulfilment of the Requirements for the Degree of Masters of Science

In

Mechanical Engineering

(Mechanical Design)

Advisor: Dr. Daniel Tilahun

Co-Advisor: Mulugeta H/Mariam

October, 2017

Addis Ababa University
Addis Ababa Institute of Technology
School of Mechanical and Industrial Engineering

Automobile Bumper Beam Analysis to Improve Energy Absorption

By

Habtamu Molla

Submitted In Accordance With the Requirements for the Degree

Master of Science (M.Sc.)

Approved By Board of Directors

Daniel Tilahun (Dr.)	_____	_____
Advisor	Signature	Date
Mulugeta H/Mariam	_____	_____
Co Advisor	Signature	Date
_____	_____	_____
Internal Examiner	Signature	Date
_____	_____	_____
External Examiner	Signature	Date
_____	_____	_____
Chairman of the School	Signature	Date

DECLARATION

Addis Ababa University

School of Graduates

This is to certify that the thesis prepared by **Habtamu Molla**, entitled: “**Automobile Bumper Beam Analysis to Improve Energy Absorption**”, do here by declare this thesis is my original work and that it has not been submitted partially, or in full for a degree in any university/institution, which compiles with the regulations of the university and meets the accepted standards with respect to originality and quality.

Signature: _____

Date: _____

Advisor: Daniel Tilahun (Dr.) Signature: _____ Date: _____

Co Advisor: Mulugeta H/Mariam Signature: _____ Date: _____

Head of School: _____ Signature: _____ Date: _____

ACKNOWLEDGEMENT

First of all, I want to thank The Almighty GOD for giving me the time and chances to finally complete this research.

And also I would like to thank my Advisor Dr. Daniel Tilahun and Co. Advisor Mr. Muluguta H/Mariam (PhD candidate) for their great effort in terms of supervision, support, dedication and patience from the every start and every detailed process until accomplishment of my research.

I would like to express my sincere gratitude to my co-advisor Mr. Muluguta H/Mariam (PhD candidate), for his invaluable guidance, continuous encouragement and constant support in making this research possible. He has always support me in times when I faced difficulties during completing this research and constantly giving the best advice to help me.

My sincere thanks go to all staff of school of Mechanical and industrial Engineering, AAiT, who helped me in many ways whenever I needed. Thanks for always putting up the best effort in helping me to finish this research.

Finally, I would like to thanks and give my appreciation to all of my family members and my friends those who were supporting and motivating me for the achievement of this study.

ABSTRACT

Automobile Bumper Beam Analysis to Improve Energy Absorption

Habtamu Molla

Addis Ababa University, 2017

Automotive Bumper is one of the main parts which is used as protection for passengers from front and rear collision. Bumpers beam play an important role in preventing the impact load from being transferred to the automobile and passengers. So it becomes an important part of a vehicle as a safety and performance point of view. The basic use of bumper is to absorb energy in case of a collision. The main purpose of this paper is to design a bumper beam which is to improve crashworthiness of the bumper and analyzes the impact behavior of a composite car bumper beam made from s-glass fiber reinforced epoxy composite materials with a volume fraction 60% fiber and 40% matrix. Crashworthiness is the ability of the bumper beam to prevent occupant injuries in the event of an accident and this is achieved by minimizing the impact force during the collision. The existing lifan 520 model bumper beam is replaced with composite bumper. The internal energy which is absorbed by steel material is 1200.9 J where the composite material is 1960 J which is 38.7 % higher than that of steel. The study is performed using ANSYS software for the design of the new car bumper made from s-glass fiber reinforced epoxy composite materials and the internal energy absorbed by the materials, total deformation as well are evaluated by use of finite element method.

Keywords: *s glass fiber, epoxy, impact load, total deformation, internal energy.*

TABLE OF CONTENTS

DECLARATION	i
ACKNOWLEDGEMENT	ii
ABSTRACT.....	iii
TABLE OF CONTENTS.....	iv
LIST OF TABLE	vi
LIST OF FIGURES	vii
NOMENCLATURE	viii
LIST OF ABBREVIATION AND ACRONYMS.....	x
CHAPTER ONE.....	1
INTRODUCTION	1
1.1. Background.....	1
1.2. Statement of Problem.....	3
1.3. Objective of the study	3
1.3.1. Specific Objectives.....	3
1.4. Scope of the Study	3
1.5. Organization of the Thesis	4
CHAPTER TWO	5
LITERATURE REVIEW	5
CHAPTER THREE	13
ANALYTICAL METHODS	13
3.1. Material.....	13
3.1.1. Glass Fibers.....	15
3.1.2. Fibers.....	18
3.1.3. Matrix.....	18
3.1.4. Epoxy Resin.....	19
3.1.4. S- GLASS FIBER	21
3.1.5. Engineering Constants of a Unidirectional Composite Lamina.....	22
3.1.5. FRP Sheet Engineering Constants from Constituent Properties	24
3.2. Methodology	28
3.3. CONDITIONS	30
3.3.1. Impact condition and tests in automotive structures	30
3.3.2. Mathematical Model Used for Dynamic Explicit Solution.....	32

3.3.3. Load Determination	35
CHAPTER FOUR.....	37
FINITE ELEMENT IMPACT SIMULATION USING ANSYS SOFTWARE.....	37
Finite Element Analysis	37
4.1. Existing Lifan 520 Model Bumper	37
4.1.1. Meshing.....	37
4.1.2. Fixed Support.....	38
4.1.3. Impact Load	39
4.2. Modified S –Glass Fiber Reinforced Epoxy Bumper Beam.....	39
4.2.1. Layered Section.....	40
4.2.2. Meshing.....	41
CHAPTER FIVE	42
RESULT AND DISCUSSION	42
5.1. Existing AISI 1006 Steel Bumper Beam Results.....	42
5.1.1. Total Deformation.....	42
5.1.2. Equivalent Elastic Strain.....	43
5.1.3. Equivalent (von –mises) stress.....	44
5.1.4. Internal Energy.....	45
5.2. Modified s glass fiber reinforced epoxy composite bumper beam	46
5.2.1. Total Deformation.....	46
5.2.2. Equivalent Elastic Strain.....	47
5.2.3. Equivalent (Von-Mises) Stress	48
5.2.4. Internal Energy.....	49
5.3. Result and discussion	50
5.3.1. Total deformation.....	50
5.3.2. Equivalent Elastic Strain.....	51
5.3.4. Internal Energy.....	51
CHAPTER SIX.....	52
CONCLUSION AND RECOMMENDATION.....	52
6.1. CONCLUSION.....	52
6.2. RECOMMENDATION	53
REFERENCES	54
APPENDIX A.....	58
APPENDIX B	59

LIST OF TABLE

Table 1.1. Summary of Literature Review.....	12
Table 2: Properties of Common Glass Fibers	18
Table 3: Properties of Thermosetting Polymers At Room Temperature	20
Table 4: General Properties of steel 1006	21
Table 5: Typical Mechanical Properties For S – Glass Fiber / Epoxy	27

LIST OF FIGURES

Figure 1: Conventional Vehicle Bumper System.	2
Figure 2: Furnace For Glass Melting.....	16
Figure 3: Fiberglass Forming Process	17
Figure 4: Existing Lifan 520 Model Steel Bumper Beam	29
Figure 5: Equivalent Spring Mass System For Bumper And Impactor	32
Figure 6: Existing Lifan 520 Model Bumper.....	37
Figure 7: Meshing	38
Figure 8: Fixed Support.....	38
Figure 9: Impact Load.....	39
Figure 10: Optimized S –Glass Fiber Reinforced Epoxy Bumper Beam	39
Figure 11: Face Surface Of The Beam.....	40
Figure 12: Layered Section	40
Figure 13: Meshing Of S Glass Fiber Reinforced Epoxy Beam Material	41
Figure 14: Total Deformation Of Steel Bumper Beam.....	42
Figure 15: Equivalent Elastic Strain	43
Figure 16: Equivalent (Von-Mises) Stress.....	44
Figure 17: Internal Energy	45
Figure 18: Total Deformation Of S Glass Fiber Reinforced Epoxy Beam Material	47
Figure 19: Equivalent Elastic Strain	48
Figure 20: Equivalent (Von-Mises) Stress.....	49
Figure 21: Internal Energy	49
Figure 22: Total Deformation Of Both Materials.....	50
Figure 23: Equivalent Elastic Strain Of Both Materials	51

NOMENCLATURE

V_m	Volume Of Matrix (Cm ³)
P_f	Density Of Fiber (Gm/Cm ³)
MM	Matrix Mass Fraction
P_m	Density Of Matrix (Gm/Cm ³)
MF	Fiber Mass Fraction
VF	Fiber Volume Fraction
M_f	Mass of Fiber (Gm)
E_i	Impact Energy (J)
E_1	Longitudinal Young's Modulus
E_2	Transverse Young's Modulus
E_f	The Fiber Modulus,
V_f	The Fiber Volume Fraction,
E_m	The Matrix Modulus
N_{12}	Major Poisson's Ratio
G_{12}	In-Plane Shear Modulus
$[M]$	Structural Mass Matrix
$\{\ddot{U}\}$	Acceleration Vector
$[C]$	Structural Damping Matrix
$\{\dot{U}\}$	Velocity Vector

[K] Structural Stiffness Matrix

{U} Displacement Vector

{F} Load Vector

LIST OF ABBREVIATION AND ACRONYMS

ASTM	American Society of Testing Materials
FEA	Finite Element Analysis
FEM	Finite Element Method
(FRP)	Fiber-Reinforced Polymer
Mph	Miles Per Hour
Min	Minute
Hr.	Hour
Cc	Cubic Centimeter
Eq.	Equation
M	Meter
Mm	Millimeter
FMSS	Federal Motor Vehicle Safety Standards
CMVSS	Canadian Motor Vehicle Safety Standards
AAIT	Adiss Ababa University Institute Of Technology

CHAPTER ONE

INTRODUCTION

1.1. Background

A bumper is a car shield made of steel, aluminum, rubber, or plastic that is mounted on the front and rear of a passenger car. When a low speed collision occurs, the bumper system absorbs the shock to prevent or reduce damage to the car. An automotive bumper is the rear most or front most part of the vehicle which is used to protect the passengers inside from the impact during a collision. [1]

One possible application area that allows material replacement to achieve vehicle light weighting is the bumper subsystem. Optimization of the car bumper subsystem, particularly the bumper beam can improve not only weight reduction but also structural energy absorption.

The bumper beam plays an important role in the energy absorption during a collision. The materials selected for automotive bumper has been recently a concern. The main governing criteria for material selection are stiffness and strength properties that will determine the overall performance of vehicle during static and dynamic loading conditions.

Fiber reinforced composite materials have been widely used in various transportation vehicle structures because of their high specific strength, modulus and high damping capability. If composite materials are applied to vehicles, it is expected that not only the weight of the vehicle is decreased but also that noise and vibration are reduced. In addition to that, composites have a very high resistance to fatigue and corrosion. Traditionally, the materials used in the construction of vehicle bodies are mainly various grades of steel. Although aluminum-intensive body concepts were used starting from executive class cars, and then later on applied to other car classes. This study focuses on the application of s - glass fiber reinforced epoxy resin composite materials in a car bumper beam for optimizing energy absorption. [2, 5]

Steel bumper beam have many advantages such as good load carrying capacity. In spite of its advantages, it stays back in low strength to weight ratio. It is reported that weight reduction with adequate improvement of mechanical properties has made composites

as a viable replacement material for conventional steel. In the present work, the steel bumper used in passenger vehicles is replaced with a very good composite polymeric based bumper. Nowadays, the composites are used mainly to make cars more energy efficient by reducing weight, together with providing durability, corrosion resistance, toughness, design flexibility, resiliency and high performance at low cost. The study is performed using ANSYS software for the design of the new car bumper made from s-glass fiber reinforced epoxy resin and the stress concentration distribution is evaluated by use of FEM to determine the impact cases.

As shown in Fig.1. A conventional bumper system comprises a bumper cover 1 defining an outer appearance of the bumper system,

an energy absorber 2 formed of an elastic material such a polypropylene foam body or an urethane foam body to absorb energy, an impact beam 3 for supporting the energy absorber 2 ,and a stay 4 for connecting the impact beam 3 to a vehicle body. [3, 4]

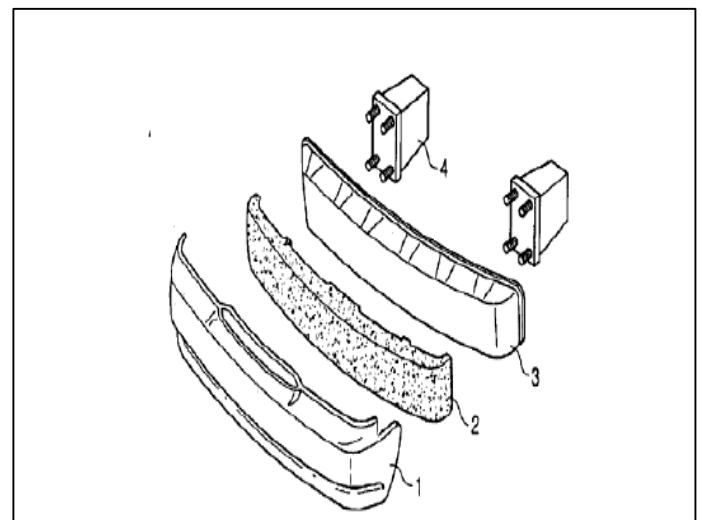
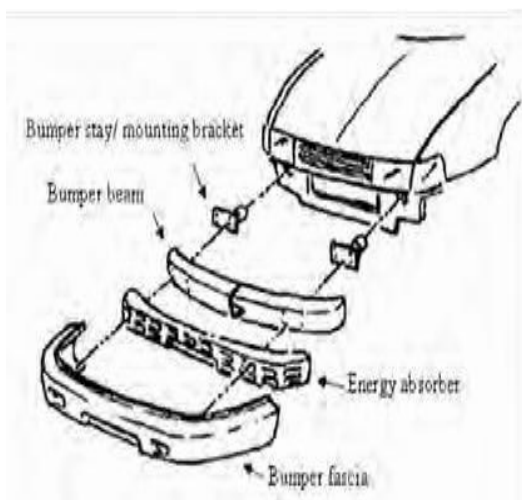


Figure 1: Conventional vehicle bumper system.

1.2. Statement of Problem

Nowadays car accidents are the main concern, passengers are dead and engine, radiator also fully damaged because of a less energy absorption capability of an impacting bumper beam. Customer also blame to the manufacture that the bumper easily to damage although the collision was slow.

1.3. Objective of the study

The general objective of this thesis is to improve automobile bumper beam energy absorption using s-glass fiber reinforced epoxy resin material for salon type vehicle.

1.3.1. Specific Objectives

- To Improve the Geometry (shape, and dimension).
- Material Improvement(proper material selection)
- To measure the energy absorbed by the materials

1.4. Scope of the Study

The study will focus on existing design performance, advantage and limitations. Based on observations design improvements will be made in terms of shape, size and or material based on design modification objectives. Modified lifan 520 model car front bumper beam design will be tested using FEM software for impact loads as per international standards.

1.5. Organization of the Thesis

This study is organized in six chapters.

Chapter one: it outlines the background, the general idea of the researches and statement of the problems, the scopes of the study, the objectives of the study as well.

Chapter two: deal with literature review from previous studies.

Chapter three: deal with analytical methods. Here determination of load and boundary condition are discussed.

Chapter four: Finite element impact simulation and procedure using ansys software was briefly discussed and presented.

Chapter five: Results from the impact simulation using ansys software are presented and discussed briefly

Chapter six: Finally the conclusion and recommendations are presented.

CHAPTER TWO

LITERATURE REVIEW

Hosseinzadeh RM and et.al [6] in their paper says that bumper beams are one of the main structures of passenger cars that protect them from front and rear collisions. In this paper, a commercial front bumper beam made of glass mat thermoplastic (GMT) is studied and characterized by impact modeling using LS-DYNA ANSYS 5.7 according to the E.C.E. UNITED NATIONS AGREEMENT [UNITED NATIONS AGREEMENT, Uniform Provisions concerning the Approval of Vehicles with regards to their Front and Rear Protective Devices (Bumpers, etc.), E.C.E., 1994]. Three main design factors for this structure: shape, material and impact conditions are studied and the results are compared with conventional metals like steel and aluminum. Finally the aforementioned factors are characterized by proposing a high strength SMC bumper instead of the current GMT.

Marzbanrad JM et.al [7] discussed the most important parameters including material, thickness, shape and impact condition are studied for design and analysis of an automotive front bumper beam to improve the crashworthiness design in low-velocity impact. The simulation of original bumper under condition impact is according to the low-speed standard of automobiles stated in E.C.E. United Nations Agreement Regulation no.42,1994. In this research, a front bumper beam made of three materials: aluminum, glass mat thermoplastic (GMT) and high-strength sheet molding compound (SMC) is studied by impact modeling to determine the deflection, impact force, stress distribution and energy-absorption behavior. The mentioned characteristics are compared to each other to find best choice of material, shape and thickness. The results show that a modified SMC bumper beam can minimize the bumper beam deflection, impact force and stress distribution and also maximize the elastic strain energy. In addition, the effect of passengers in the impact behavior is examined.

Different countries have different performance standards for bumpers. Under the International safety regulations originally developed as European standards and now

adopted by most countries outside North America, a car's safety systems must still function normally after a straight-on pendulum or moving-barrier impact of 4 km/h (2.5 mph) to the front and the rear, and to the front and rear corners of 2.5 km/h (1.6 mph) at 45.5 cm (18 in) above the ground with the vehicle loaded or unloaded. In North America (FMSS: Federal Motor Vehicle Safety Standards) and Canada (CMVSS: Canadian Motor Vehicle Safety Standards), it should be meet 4KMPH pendulum and barrier impacts. [8]

Mohapatra S [9] discusses that automotive development cycles are getting shorter by the day. With increasing competition in the marketplace, the OEM's and suppliers main challenge is to come up with time-efficient design solutions. Researchers are trying to improve many of existing designs using novel approaches. Many times there is conflicting performance and cost requirements, this puts additional challenge with R&D units to come up with a number of alternative design solutions in less time and cost compared to existing designs. These best solutions are best achieved in a CAE environment using some of the modern CAD and FEM tools. Such tools are capable of effecting quick changes in the design within virtual environment.

A bumper is a car shield made of steel, aluminum, rubber, or plastic that is mounted on the front and rear of a passenger car. When a low speed collision occurs, the bumper system absorbs the shock to prevent or reduce damage to the car. Some bumpers use energy absorbers or brackets and others are made with a foam cushioning material. The car bumper is designed to prevent or reduce physical damage to the front and rear ends of passenger motor vehicles. Generally, a bumper is attached to either end of a vehicle to absorb impact in a collision, thereby protecting passenger.

Andersson R et.al [10] disclosed is a bumper system including a bumper cover, an energy absorber formed of a synthetic resin material through a foam molding process, an impact beam for supporting the energy absorber, the impact beam being formed of a glass mat thermoplastic ssand having a "C"-shaped section, and a stay for connecting the impact beam to a vehicle body. Tips are formed on front upper and lower portions of the impact beam, and a web portion is formed on the impact beam between the tips. Tip insertion grooves in which the tips are inserted are formed on an inner surface of the energy absorber,

and a pressure receiving surface corresponding to the web portion is formed on the inner surface of the energy absorber.

Butler M et.al [11] focuses that to increase crash performance in automotive vehicles it is necessary to use new techniques and materials. Components linked to crash safety should transmit or absorb energy. The energy absorbing capability of a specific component is a combination of geometry and material properties. For these components the chosen material should have high yield strength and relatively high elongation to fracture. These demands have led to increasing interest in the use of high strength stainless steels.

Carley ME et.al [12] the objective of this study is to design efficient epoxy structural foam reinforcements to improve the energy absorption of front and rear automotive bumper beams. Three bumper structural performance criteria were studied.

Evans D and Morgan T [13] as vehicle manufacturers continue to become more aggressive with the styling of new vehicles, bumper system technologies will be required to find new solutions that fit into the reduced package spaces while continuing to meet the vehicle performance and cost requirements. The purpose of this paper is to introduce new and innovative Expanded Polypropylene (EPP) foam technologies and techniques.

Witteman WJ [14] automotive styling trends point to reduced bumper overhang, greater sweeps, and reduced overall package space for the bumper system. This paper will review the industry trends associated with bumper energy absorbers and explore the potential fit of this new prototype energy absorber design as an alternative to EPP foam. Also included is a review of the simulated performance of the prototype ETP energy absorber and a comparison of its actual test results for 8 km / h FMVSS Part 581 impact series to the performance of EPP foam packaged in the same environment.

Masoumi A et.al [15] in their thesis describes the design of a new frontal vehicle structure that directs the asymmetric crash load of an offset collision as an axial load to the second unloaded longitudinal member. Only by using both longitudinal members and through a progressive folding pattern, enough energy can be absorbed in the front structure to prevent a deformation of the passenger compartment. To prevent a premature bending collapse, the new longitudinal members consist of two functional components: an inside

square crushing column for a normal stable axial force level and a stiff outside sliding supporting structure that gives the necessary extra bending resistance. An integrated cable system transmits the force to the other longitudinal member. With this novel design concept, a vehicle has similar energy absorption in the front structure for the entire range of collision situations (full, offset, oblique).

Zonghua Zhang, Shutian Liu, Zhiliang Tang [16] discusses that material selection for automotive closures is influenced by different factors such as cost, weight and structural performance. Among closures, the automotive bonnet must fulfill the requirements of pedestrian safety which is evaluated by child and adult headform impactors. The mechanisms of injury are complex, therefore; the Head Injury Criterion (HIC) which shows a measure of the likelihood of head injury arising from an impact is developed. HIC includes the effects of head acceleration and the duration of the acceleration. In this paper a new finite element model has been developed which is capable to simulate head impact phenomenon between headform impactors and composite bonnet. Then the behavior of three identical bonnets made of steel, aluminum and composite have been investigated by the developed model.

In this paper, O. G. Lademo et.al [17] discusses about a rib-reinforced thin-walled hollow tube-like beam (named as rib-reinforced beam) is presented for potential application in vehicle bumper. Through numerical simulation of the bending behavior under impact loads, the rib-reinforced beam is compared with thin-walled hollow tube-like beams filled with and without foam materials (empty beam and foam-filled beam) in crashworthiness. The effects of the shape of the reinforced rib are investigated and the shape optimization design is performed for increasing energy absorption and reducing the initial peak force. A multi-objective crashworthiness optimization formulation including maximum energy absorption, maximum specific energy absorption and minimum initial peak force is constructed based on the ideal point method (IPM). The optimum configuration of the reinforced rib is given with a normalized cubic spline function. Numerical example results show that, compared with the empty and foam-filled beams with same weights, the optimized rib-reinforced beam has higher energy absorption performance and lower initial crash force. It is found that for the rib-reinforced beam little rumples are formed around the

compressed indentation, which helps to retard the collapse of the side wall and means more energy absorption.

Nitin S. Gokhale, Sanjay S.Despande, Dr. Anand N. Thite [18] Manufacturing of a bumper system from aluminum extrusions often involves series of forming operations performed in the soft W-temper condition, and then artificially age-hardening of the components to the material's peak hardness T6 condition. It is probable that proper finite element (FE) modeling of the crash performance of the resulting systems must rely upon a geometry obtained from an FE model following the process route, i.e., including simulation of all major forming operations. The forming operations also result in an inhomogeneous evolution of some internal variables (among others the effective plastic strain) within the shaped components. Results from tensile tests reveal that plastic straining in W-temper leads to a significant change of the T6 work-hardening curves. In addition, the tests show that the plastic pre- deformation causes a reduction of the elongation of the T6 specimens. In the present work, these process effects have been included in a user- defined elastoplastic constitutive model in LS-DYNA incorporating a state-of-the-art anisotropic yield criterion, the associated flow rule and a non-linear isotropic work hardening rule as well as some ductile fracture criteria.

Ramazan Karakuz, Emre Erbil and Mehmet Aktas [2010] [19] are conducted the research on the damage prediction in glass/epoxy laminates subjected to low velocity impact loading using both numerical simulation and experimental laboratory analysis. The experimental laboratory test was done by using Fractovis plus impact testing machine using 20 J of impact energy. In their paper the impact behavior of unidirectional laminated glass/epoxy composite plates with $[0/\pm\theta/90]_s$ fiber orientation is investigated numerically equal energy of 40J, equal velocity 2m/s and equal impactor mass 5kg. In order to examine the stacking effect, they chose five different $\pm\theta$ fiber directions (15° , 30° , 45° , 60° and 75°). Three different plate thicknesses at 2.9 mm, 5.8 mm, and 8.7 mm are also selected to survey the thickness effect on impact behavior of glass/epoxy composite plates. A transient finite element code 3D IMPACT is used for numerical analyses in order to calculate the stress and contact forces according to composite plate during impact events. It can also be used for predicting the threshold of impact damage and initiation using choi and chang failure/damage criteria. In this code an eight- point brick element and the direct gauss

quadrature integration scheme are used by authors through the element thickness to account for the change in material properties from layer to layer. The Newmark scheme is also adopted to perform time integration step by step. In addition a contact law incorporated with the newton Raphson method is applied to calculate the contact forces during impact. Finally the researchers are compared the numerical results with the experimental study and it conclude that they are in good agreement with the experimental results.

The thermo physical properties of natural fiber reinforced polyester composites are carried out by **Idicula et al** [20] . They have identified that the incorporation of natural fiber with glass fiber improves the heat transport ability of the composite materials significantly. **Cicala et al** have studied the properties and performances of various hybrid glass/natural fiber composites for the applications in curved pipes. **Arbelaiz et al** evaluated the mechanical properties of flax fiber/polypropylene composites and studied the influence of fiber/matrix modification and glass fiber hybridization. They have reported that the tensile strength and modulus of hybrid glass/flax polypropylene composites depend on the glass/flax ratio.

Thwe and Liao [21, 56] have analyzed the ability of bamboo and glass fiber reinforced polymer matrix hybrid composites and reported that there is a significant improvement due to the incorporation of bamboo fibers with glass fiber. The properties such as tensile strength and elastic modulus of bamboo fiber reinforced polypropylene and bamboo glass fiber reinforced polypropylene hybrid composites have been evaluated. The results indicated that the tensile strength and elastic modulus decreased after ageing of fibers. The overall tensile and flexural properties of natural fiber reinforced polymer hybrid composites are highly dependent on the aspect ratio, moisture absorption tendency, morphology and dimensional stability of the fibers used. The tensile strength and modulus of short, randomly oriented hybrid natural fiber composite are found out by experimentally and comparing the results by using rule of hybrid mixture (RoHM).

Summary of Literature Review

	Author	Year	Title	Journal	Findings
1	Witteaman WJ	2000	Improved Vehicle Crashworthiness Design by Control of the Energy Absorption for Different Collision Situations	Doctoral dissertation, Eindhoven University of Technology	This paper addresses an alternative to the bumper energy absorber systems
2	Andersson R, Schedin E, Magnusson C, Ocklund J	2002	The Applicability of Stainless Steel for Crash Absorbing Components	SAE Technical Paper	The impact beam being formed of a glass mat thermoplastic and having a "C"-shaped section, and a stay for connecting the impact beam to a vehicle body.
3	Butler M, Wycech J, Parfitt J, and Tan E	2002	Using Terocore Brand Structural Foam to Improve Bumper Beam Design	SAE Technical Paper	In this work energy absorbing capability of a specific component is a combination of geometry and Material properties are discussed.
4	Carley ME, Sharma AK, Mallela V	2004	Advancements in expanded polypropylene foam energy management for bumper systems	SAE Technical Paper	Design efficient epoxy structural foam reinforcements to improve the energy absorption of front and rear automotive bumper beams.
5	Hosseinzadeh RM, Shokrieh M, and Lessard LB	2005	Parametric study of automotive composite bumper beams subjected to low-velocity impacts	Journal of Composite Structure	In this paper, a commercial front bumper beam made of glass mat thermoplastic (GMT) is studied and characterized by impact modeling using LS-DYNA ANSYS 5.7
6	Mohapatra S	2005	Rapid Design Solutions for Automotive Bumper Energy Absorbers using Morphing Technique	Altair CAE users Conference 2005, Bangalore, India	Impact Analysis of a car shield made of steel, aluminum, rubber, or plastic of a passenger car at low Collision speed.
7	O. G. Lademo, T. Berstad, M. Eriksson, T. Tryland, T. Furuc, O. S. Hopperstad, M. Langseth,	2008	A model for process-based crash simulation	Norwegian University of Science and Technology Trondheim, Norway	Discussed a rib-reinforced thin-walled hollow tube-like beam (named as rib-reinforced beam) is presented for potential application in vehicle bumper.
8	Zonghua Zhang, Shutian Liu, Zhiliang Tang	2009	“Design optimization of cross-sectional configuration of rib-reinforced thin-walled beam”	Dalian University of Technology, Dalian, China.	Discusses that material selection for automotive closures is influenced by different factors such as cost, weight and structural performance

9	Marzbanrad JM, Alijanpour M, and Kiasat MS	2009	Design and analysis of automotive bumper beam in low speed frontal crashes	Thin Walled Structure	Discusses the important Parameter including material,thickness,shape and impact condition are studied for design and analysis of an automotive front bumper beam to improve the crashworthiness design in low-velocity impact.
10	Masoumi A, Mohammad Hassan Shojaeefard,	2011	Comparison of steel, aluminum and composite bonnet in terms of pedestrian	College of Engineering, University of Tehran,	Describes the design of a new frontal vehicle structure that directs the asymmetric crash load of an offset collision as an axial

Table 1. Summary of Literature Review

Research gap in previous investigation

Many researchers has been done on the low speed collision which is done by pendulum test, and Some researchers have been done on the bumper fascia and energy absorber rather than the reinforcing beam in order to improve the energy absorption. There is a lack of researches on the moderate speed impact analysis. On the whole, after evaluating all the concerned books and research work, a conclusion can be made that the safety of the passenger needs to be increased.

CHAPTER THREE

ANALYTICAL METHODS

3.1. Material

Determining the right material during the selection process is very important. The material selected should meet the expectation of the engineer. The material should prove mechanically feasible and should be economical. Apart from this the selected material must convincingly prove better than the currently used material. The proposed material properties may help the material engineers to perform the right material selection during the selection stage. [22]

The selection of material for automotive bumper depends on the following factors.

Energy Absorption (EA)

One of the key factors in the selection of material for bumpers is the ability of the material to absorb the kinetic energy of collision. This ability of the material to absorb energy is called impact toughness. Impact toughness is defined as a measure of the ability of the material to absorb energy during impact.

Performance

Performance is defined as the ability of the material to stay rigid during an impact. The two factors that determine the performance are the flexural strength and flexural modulus.

Flexural Strength is defined as the ability of a material to withstand failure due to bending. **Flexural Modulus** is defined as the capability of the material to resist bending or deflection. The flexural strength is also known as stiffness of the material.

Cost

Cost determines the feasibility of the use of a material for automotive bumpers. The cost of a material makes it preferable for the industrial application. The cost of these composite materials should be less than that of the standard materials used in the automotive bumpers. Also it should be noted that the reduction of cost should not account for the reduction in performance and quality of the bumper.

Weight

One of the primary reasons for the engineers to check for new type of materials is the weight reduction factor. The reduction of weight plays an important role in the fuel consumption. By reduction in weight, we mean that the reduction in dead weight of vehicle. Decreasing the dead weight on the engine ensures that less power is required for the constant load hence lowers the fuel consumption. Therefore reduction in weight of any component of a vehicle reduces the net dead weight.

Service Conditions

As the bumper is exposed to different kind of weather, the engineers must make sure that the bumper material should be resistant to different kind of weather conditions. The two material properties that have to be considered for the bumper material are resistant to corrosion and water absorption. As the name suggests resistant to corrosion is the ability of the material to resist corrosion. Water absorption is defined as the amount of water absorbed by a material.

Manufacturing Process

The manufacturing process necessary are also needed to be considered while selecting the best material for the product development process. One of the main factors that has to be considered is the shape of the bumper. It should be noted that the bumper material should provide the ease of changing the shape to the required design. Manufacturing process includes the selection of the best process either forming or shaping in order to achieve the required design.

Availability of the material

Availability of the material can be categorized into two; namely the availability of the raw materials and the information regarding the raw materials. The information regarding the materials is a must for the designers during the design process.

Environment Considerations

Due to the depletion an increasing demand of the natural source of minerals and metals, it has been a greater concern to the environmentalist. Therefore it is important for to select of materials that can be recycled and has longer life.

3.1.1. Glass Fibers

Glass Fibers are among the most versatile industrial materials known today. They are readily produced from raw materials, which are available in virtually unlimited supply. Glass fiber is made by blending raw materials, melting them in a three-stage furnace, extruding the molten glass through bushings in the bottom of the fore hearth, cooling the filaments with water, and then applying a chemical size. The filaments then are gathered and wound into a package. All glass fibers described in this article are derived from compositions containing silica. They exhibit useful bulk properties such as hardness, transparency, resistance to chemical attack, stability, and inertness, as well as desirable fiber properties such as strength, flexibility, and stiffness. Glass fibers are used in the manufacture of structural composites, printed circuit boards and a wide range of special-purpose products. Over 95% of the fibers used in reinforced plastics are glass fibers, as they are inexpensive, easy to manufacture and possess high strength and stiffness with respect to the plastics with which they are reinforced. Their low density, resistance to chemicals, insulation capacity are other bonus characteristics, although the one major disadvantage in glass is that it is prone to break when subjected to high tensile stress for a long time.. [23]

Fiber Forming Processes Glass melts are made by fusing (co-melting) silica with minerals, which contain the oxides needed to form a given composition. The molten mass is rapidly cooled to prevent crystallization and formed into glass fibers by a process also known as fiberization. Nearly all continuous glass fibers are made by a direct draw process and formed by extruding molten glass through a platinum alloy bushing that may contain up to several thousand individual orifices, each being 0.793 to 3.175 mm (0.0312 to 0.125 in.) in diameter . While still highly viscous, the resulting fibers are rapidly drawn to a fine diameter and solidify. Typical fiber diameters range from 3 to 20) μm (118 to 787) μm . Individual filaments are combined into multifilament strands, which are pulled by mechanical winders at velocities of up to 61 m/s (200 ft/s) and wound onto tubes or forming packages. This is the only process that is described in detail subsequently in the present article.

The marble melt process can be used to form special-purpose, for example, high-strength fibers. In this process, the raw materials are melted, and solid glass marbles, usually 2 to 3

em (0.8 to 1.2 in.) in diameter, are formed from the melt. The marbles are remelted (at the same or at a different location) and formed into glass fibers. [24]

Sizes and Binders. Glass filaments are highly abrasive to each other. "Size" coatings or binders are therefore applied before the strand is gathered to minimize degradation of filament strength that would otherwise be caused by filament-to-filament abrasion. Binders provide lubrication, protection, and/or coupling. The size maybe temporary, as in the form of a starch-oil emulsion that is subsequently removed by heating and replaced with a glass-to-resin coupling agent known as a finish. On the other hand, the size may be a compatible treatment that performs several necessary functions during the subsequent forming operation and which, during impregnation, acts as a coupling agent to the resin being reinforced. [25]

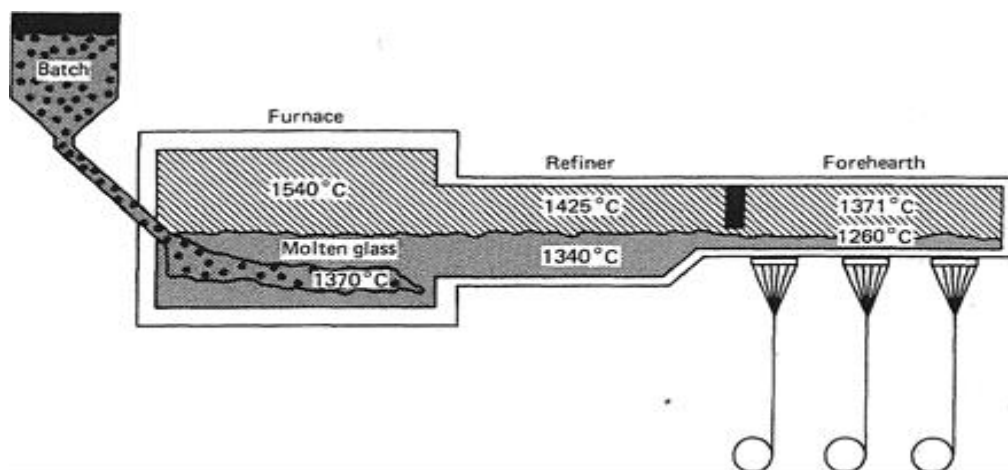


Figure 2: Furnace for Glass Melting

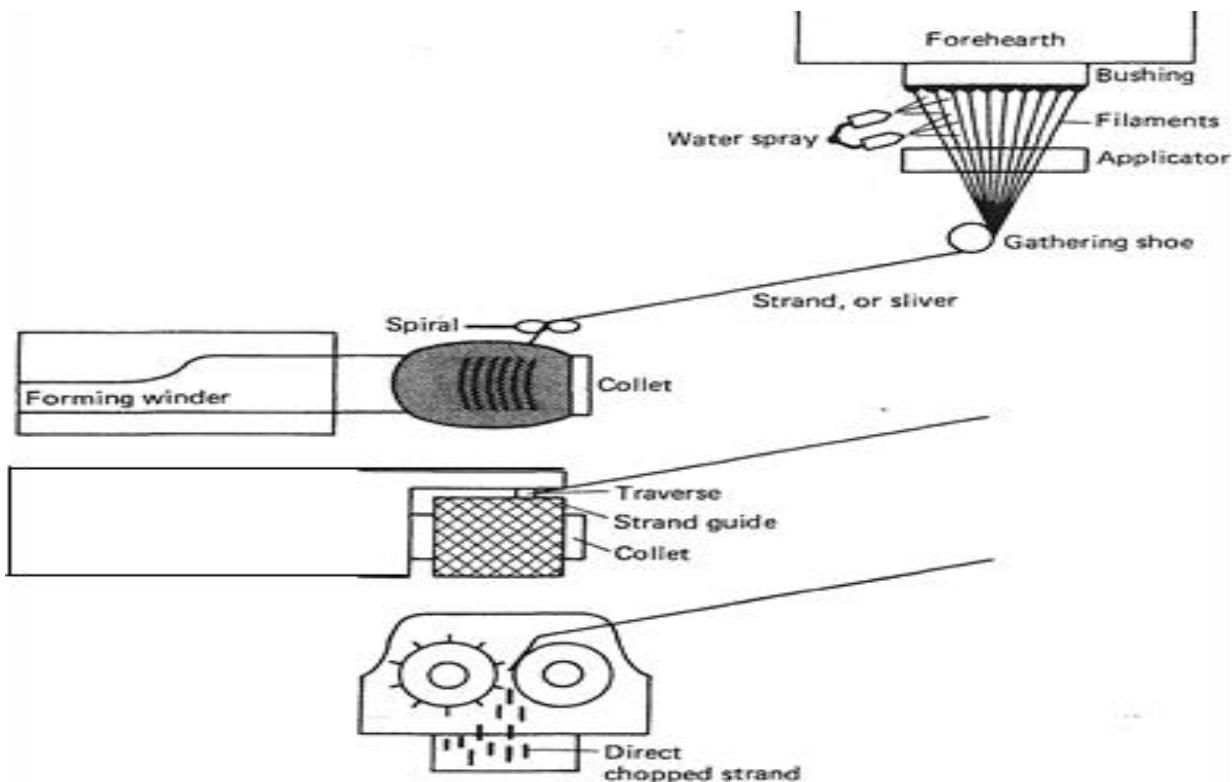


Figure 3: Fiberglass Forming Process

Fiber-reinforced polymer (FRP) is composed of two material phases: fiber and polymer matrix. Fibers are impregnated into the polymer matrix to form a macroscopically orthotropic layer of material with distinctly higher mechanical properties along the fiber direction compared to the transverse directions. The advantages of using FRP are the high strength and stiffness-to-weight ratio along the fiber direction, ease of application in construction due to its light weight, corrosion resistance, electromagnetic inertness, and design versatility in which high strength and stiffness (fibers) may be oriented where needed in design. Continuous fibers become extremely strong and stiff as fiber diameter becomes smaller due to the reduction and sometimes elimination of defects in the microstructure. On the other hand, small-diameter fibers are not capable of carrying axial compression or shear stresses due to the lack of shear transfer medium between them. [26] Thus, the fibers are embedded into a

polymeric matrix that binds them together and allows load transfer by shear among the fibers. Additional specifics about fibers and matrix are described in the following sections.

3.1.2. Fibers

Fibers are typically made of glass, carbon, and aramid. Other synthetic fibers are made of polymers which are not used in structural applications due to their low mechanical properties. Glass fibers are primarily composed of silicon dioxide with some modifying agents (Gibson 1994). E-glass (electrical glass) accounts for the largest production of glass fibers in industry due to its low cost despite its mechanical properties that are lower than other grades of glass fibers. On the other hand, S-glass (structural glass) is more expensive to produce, but it has significantly higher strength and slightly higher modulus, (Gibson 1994) and (Hyer 1998). C-glass (chemical glass) has an improved durability against alkali and acid attacks. [27]

Properties of common glass fibers

Property	Glass type		
	E	C	S
Diameter (μm)	8 -14	---	10
Density (kg/m ³)	2540	2490	2490
Tensile modulus (Gpa)	72.4	68.9	85.5
Tensile strength (Mpa)	3450	3160	4590
Elongation (%)	1.8-3.2	4.8	5.7
Coeff.of thermal expansion (*10 ⁻⁶ /°C)	5.0	7.2	5.6
Thermal conductivity (w/m/°C)	1.3	--	---
Specific heat (J/kg/°k)	840	780	940

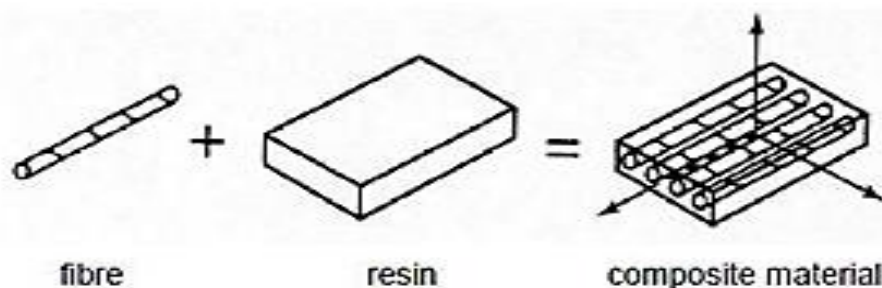
Table 2: Properties of Common Glass Fibers

3.1.3. Matrix

The matrix in a composite plays various roles such as holding the fibers into the composite part shape, protecting fibers from direct exposure to the environment, transferring the stresses through the fiber–matrix interface to the fibers, and resisting some of the applied load, especially transverse normal stresses and interlinear shear stresses (Barbers 2011). The application of a composite is limited by the properties of its matrix.

3.1.4. Epoxy Resin

The epoxide functional group is enclosed in the epoxy that is a preserved thermoset resin. Before use, the hardener (which cures epoxy resin) and epoxy resin are usually blended together. Many industries observe the use of Epoxy, e.g., structural adhesives electronic and electrical components, metal coatings, fiber-reinforced plastic materials and high tension electrical insulators. Epoxy resins are the prevalent polymer used with advanced composites. Their extensive use is primarily due to their superior mechanical properties, excellent adhesion, good possibility utilizing addition-type reactions, low cure shrinkage and low cost.



Thermosetting resins are formed into a polymer matrix through an irreversible cross-linking chemical process called resin curing. These resins are the most commonly used polymer system. This is due to the fact that they have low viscosity, allowing thorough fiber immersion, and they require low processing temperatures and short processing time. Thermoset polymers are polymers that are cured into a solid form and cannot be returned to their original uncured form. Composites made with thermoset matrices are strong and have very good fatigue strength. They are extremely brittle and have low impact-toughness making. They are commonly used for high-heat applications because the thermoset matrix doesn't melt like thermoplastics. Thermoset composites are generally cheaper and easier to produce because the liquid resin is very easy to work with. Thermoset composites are difficult to recycle because the thermoset cannot be remolded or reshaped; only the reinforcing fiber used can be reclaimed. They also cost less than thermoplastic resins (Hyer 1998). Resin shelf life refers to the amount of time that a resin system can be stored without degradation prior to mixing (Barbero 2011). Resin pot life is the time span during which mixed resin is still workable and applicable (Barbero 2011). The properties of various widely used thermosetting resins are listed (Hyer 1998). [28]

Properties of Thermosetting Polymers at Room Temperature

property	polyester	Vinyl ester	epoxy	Bismaleimide	polyimide
Density(kg/m ³)	1100-1500	1150	1100-1400	1320	1430-1890
Tensile modulus(Gpa)	1.2-4.5	3-4	2-6	3.6	3.1-4.9
Shear modulus(Gpa)	0.7-2	-	1.1-2.2	1.8	-
Tensile strength(Mpa)	40-90	65-90	35-130	48-78	70-120
Compressive strength(Mpa)	90-250	127	100-200	200	-
Elongation (%)	2-5	1-5	1-8.5	1-6.6	1.5-3
Coeff.of thermal expansion(*10e-6/°c	60-200	53	45-70	49	90
Thermal conductivity(W/m/°c)	0.2	-	0.1-0.2	-	-
specific heat(J/Kg/K)	-	-	1250-1800	-	-
Glass transition temprature (°c)	50-110	100-150	50-250	250-300	230-320
Water absorption (%) [24h@20°c]	0.1-0.3	-	0.1-0.4	-	0.3
Shrinkage on curing (%)	4-12	1-6	1-5	-	-

Source: courtesy of hyper (1998).

Table 3: Properties of Thermosetting Polymers at Room Temperature

3.1.4. S- GLASS FIBER

S-glass consists of magnesium-aluminosilicate and is generally used as reinforcement in structural applications that requires high strength and durability under high temperatures and in corrosive environments. [38]

3.1.4.1. AISI 1006 Steel

Steels containing mainly carbon as the alloying element are called carbon steels. They contain about 0.4% silicon and 1.2% manganese. Chromium, nickel, aluminium, copper and molybdenum are also present in small quantities in the carbon steels.

The features of AISI 1006 carbon steel are mainly softness and ductility. The following datasheet will provide more details about AISI 1006 carbon steel.

Property	Value
Density	7896 Kg/m ³
Yield Strength	350 MPa
Hardening Constant	275 MPa
Hardening Exponent	0.36
Strain rate constant	0.022
Melting Temperature	1538 0C
Shear Modulus	81.8 GPa
Specific Heat	452 J/Kg

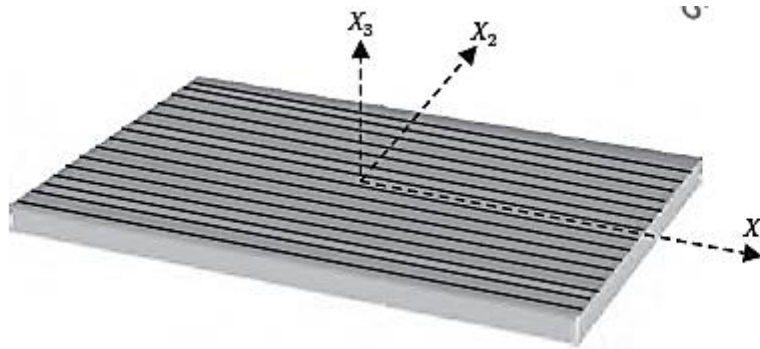
Table 4: General Properties of steel 1006

Applications

AISI 1006 carbon steel is primarily used in applications which require hard bending and welding such as panels for appliances or automobiles. AISI 1006 steel can also be used in magnet core applications.

3.1.5. Engineering Constants of a Unidirectional Composite Lamina

Unlike isotropic materials that have similar properties in all directions, a uniaxial lamina is orthotropic, with distinct properties along the fiber, transverse, and through-the-thickness directions, as seen below.



Isotropic materials have only two independent engineering constants, which are Young’s modulus of elasticity (E) and Poisson’s ratio (ν). Conversely, orthotropic laminas have nine distinct engineering parameters, including three Young’s moduli along the three principal materials directions (E_1, E_2, E_3), three independent Poisson’s ratios ($\nu_{12}, \nu_{13}, \nu_{23}$), and three shear moduli (G_{12}, G_{13}, G_{23}). The generalized 3-D compliance relationship of an orthotropic sheet is:

$$\begin{Bmatrix} \epsilon_{11} \\ \epsilon_{22} \\ \epsilon_{33} \\ \circ_{12} \\ \circ_{13} \\ \circ_{23} \end{Bmatrix} = \begin{bmatrix} \frac{1}{E_1} & -\frac{\nu_{21}}{E_2} & -\frac{\nu_{31}}{E_3} & 0 & 0 & 0 \\ -\frac{\nu_{21}}{E_1} & \frac{1}{E_2} & -\frac{\nu_{32}}{E_3} & 0 & 0 & 0 \\ -\frac{\nu_{13}}{E_1} & -\frac{\nu_{23}}{E_2} & \frac{1}{E_3} & 0 & 0 & 0 \\ 0 & 0 & 0 & \frac{1}{G_{12}} & 0 & 0 \\ 0 & 0 & 0 & 0 & \frac{1}{G_{13}} & 0 \\ 0 & 0 & 0 & 0 & 0 & \frac{1}{G_{23}} \end{bmatrix} \begin{Bmatrix} \sigma_{11} \\ \sigma_{22} \\ \sigma_{33} \\ 12 \\ 13 \\ 23 \end{Bmatrix}$$

Where $\frac{\nu_{ij}}{E_i} = \frac{\nu_{ji}}{E_j}$. The stiffness matrix is obtained by inverting the compliance matrix in (eq.3.1) (Rasheed 1996)

$$\begin{Bmatrix} \sigma_{11} \\ \sigma_{22} \\ \sigma_{33} \\ \circ_{12} \\ \circ_{13} \\ \circ_{23} \end{Bmatrix} = \begin{bmatrix} \frac{1-v_{23}v_{32}}{\Delta} E1 & \frac{v_{21}+v_{31}v_{23}}{\Delta} E1 & \frac{v_{31}+v_{21}v_{3}}{\Delta} E1 & 0 & 0 & 0 \\ \frac{v_{21}+v_{31}v_{23}}{\Delta} E1 & \frac{1-v_{13}v_{31}}{\Delta} E2 & \frac{v_{32}+v_{12}v_{31}E2}{\Delta} & 0 & 0 & 0 \\ \frac{v_{31}+v_{21}v_{32}}{\Delta} E1 & \frac{v_{32}+v_{12}v_{31}}{\Delta} E2 & \frac{1-v_{21}v_{12}}{\Delta} E3 & 0 & 0 & 0 \\ 0 & 0 & 0 & G12 & 0 & 0 \\ 0 & 0 & 0 & 0 & G13 & 0 \\ 0 & 0 & 0 & 0 & 0 & G23 \end{bmatrix} \quad \text{Eq. 3.1.}$$

$$\begin{Bmatrix} 11 \\ 22 \\ 33 \\ \gamma_{12} \\ \gamma_{13} \\ \gamma_{23} \end{Bmatrix}$$

where $\Delta = 1 - v_{12}v_{21} - v_{23}v_{32} - v_{13}v_{31} - 2v_{21}v_{32}v_{13}$.

Eq .3.2.

If the compliance matrix in Equation (3.1) is reduced to 2-D behavior (sheet analysis), the stress components $\sigma_{33} = \tau_{13} = \tau_{23} = 0$. The third, fifth, and sixth rows and columns are removed, yielding

$$\begin{Bmatrix} \epsilon_{11} \\ \epsilon_{22} \\ \circ_{12} \end{Bmatrix} = \begin{bmatrix} \frac{1}{E_1} & -\frac{v_{21}}{E_2} & 0 \\ -\frac{v_{12}}{E_1} & \frac{1}{E_2} & 0 \\ 0 & 0 & \frac{1}{G_{12}} \end{bmatrix} \begin{Bmatrix} \sigma_{11} \\ \sigma_{22} \\ 12 \end{Bmatrix}$$

Eq .3.3

The 2-D compliance matrix in Equation (3.3) may be inverted to yield the 2-D stiffness matrix (Jones 1975),

$$\begin{Bmatrix} \sigma_{11} \\ \sigma_{22} \\ \circ_{12} \end{Bmatrix} = \begin{bmatrix} \frac{E1}{1-v_{12}v_{21}} & \frac{v_{12}E2}{1-v_{12}v_{21}} & 0 \\ \frac{v_{21}E1}{1-v_{12}v_{21}} & \frac{E2}{1-v_{12}v_{21}} & 0 \\ 0 & 0 & G12 \end{bmatrix} \begin{Bmatrix} \epsilon_{11} \\ \epsilon_{22} \\ 12 \end{Bmatrix} \quad \text{Eq. 3.4.}$$

3.1.5. FRP Sheet Engineering Constants from Constituent Properties

Using the mechanics-of-materials approach requires certain simplifying assumptions in order to derive the mechanical properties of a unidirectional composite sheet. The accuracy of the estimated property depends on the accuracy of the assumption made.

a) Determination of E_1

The first modulus along the fiber direction may be determined by the rule of mixtures that results from the assumption of having the fiber and the matrix deform in equal amounts along the fiber direction (Jones 1975). This assumption is known to be very accurate, leading to an accurate estimation of the apparent Young's modulus E_1 ,

$$E_1 = E_f V_f + E_m V_m \quad (3.5)$$

Where E_f is the fiber modulus, V_f is the fiber volume fraction, E_m is the matrix modulus, and $V_m = 1 - V_f$.

b) Determination of E_2

The second modulus along the transverse direction is not as straightforward to derive. One simplifying assumption can be made considering the same transverse stress σ_2 in the fiber and the matrix, leading to the following mechanics-of-materials expression, which is known to yield a lower bound value of the apparent Young's modulus E_2 :

$$E_2 = \frac{E_f E_m}{V_m E_f + V_f E_m} \quad \text{or} \quad \frac{1}{E_2} = \frac{V_m}{E_m} + \frac{V_f}{E_f} \quad (3.6)$$

More accurate determination of E_2 could be obtained using the Halpin-Tsai equations (Jones 1975),

$$\frac{E_2}{E_m} = \frac{1 + \xi^\circ V_f}{1 - \circ V_f} \quad (3.7)$$

where

$$\eta = \frac{E_f/E_m - 1}{E_f/E_m + \xi} \quad (3.8)$$

The value of ξ could be difficult to obtain, since it is a function of the fiber geometry, packing geometry, and loading conditions. However, studies have shown that a value of $\xi = 2$ can be approximated for calculating E_2 with a fiber volume fraction of 0.55 (Jones 1975). However, $\xi = 1$ has been observed to yield more accurate results when computing typical properties.

c) Determination of ν_{12}

The major Poisson's ratio ν_{12} may be determined by the rule of mixtures resulting from the previous two assumptions of having the fiber and the matrix deform in equal amounts along the fiber direction and having the transverse stress $\sigma_2 = 0$ (Jones 1975). These assumptions are known to be accurate, leading to an accurate estimation of the major Poisson's ratio ν_{12} :

$$\nu_{12} = \nu_f V_f + \nu_m V_m \quad (3.9)$$

d) Determination of G_{12}

The sheet in-plane shear modulus G_{12} is determined in the mechanics-of-materials approach using the assumption that the shearing stress of the fiber and the matrix are identical. The well-known nonlinear shear stress–strain is linearized using this assumption. Accordingly, the resulting equation yields a lower bound solution to the in-plane shear modulus G_{12} :

$$G_{12} = \frac{G_f G_m}{V_m G_f + V_f G_m} \quad \text{or} \quad \frac{1}{G_{12}} = \frac{V_m}{G_m} + \frac{V_f}{G_f} \quad (3.10)$$

$$G_f = \frac{E_f}{2(1+\nu_f)} \quad (3.11)$$

$$G_m = \frac{E_m}{2(1+\nu_m)} \quad (3.12)$$

More-accurate determination of G_{12} could be obtained using the Halpin-Tsai equations (Jones 1975),

$$\frac{G_{12}}{G_m} = \frac{1+\xi^\circ V_f}{1-\circ V_f} \quad (3.13)$$

where

$$\eta = \frac{G_f/G_m - 1}{G_f/G_m + \xi} \quad (3.14)$$

The value of ξ could be difficult to obtain, since it is a function of the fiber geometry, packing geometry, and loading conditions. However, studies have shown that a value of $\xi = 1$ for calculating G_{12} can be approximated for a fiber volume fraction of 0.55 (Jones 1975).

e) Determination of ν_{21} :

Once the first three parameters are estimated, the minor Poisson's ratio ν_{21} is directly calculated,

$$\frac{\nu_{12}}{E_1} = \frac{\nu_{21}}{E_2} \circ \quad \nu_{21} = \frac{\nu_{12}}{E_1} E_2 \quad \text{eq. 3.15}$$

Typical mechanical properties for s – glass fiber / epoxy

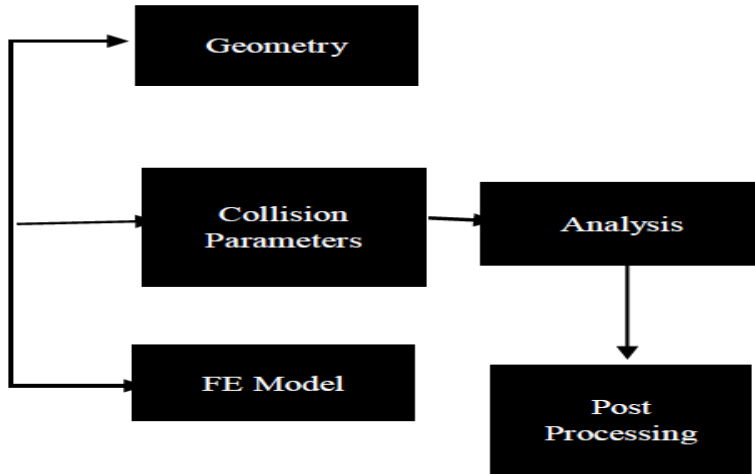
Unidirectional composites with $V_f = 0.6$

Elastic constants	GPa	10⁶ psi
Longitudinal modulus	55	8.0
Transverse modulus	16	2.3
Axial shear modulus	7.6	1.1
Poission's ratio (dimention less)	0.28	0.28
Strength properties	MPa	10³ psi
Longitudinal tension	1620	230
Longitudinal compression	690	100
Transverse tension	40	7
Transverse compression	140	20
In plane shear	80	12
Interlaminar shear	80	12
Ultimate strains	%	
Longitudinal tension	2.9	
Longitudinal compression	1.3	
Transverse tension	0.4	
Transverse compression	1.1	
In plane shear	1-6	
Density (kg/m3)	2000	

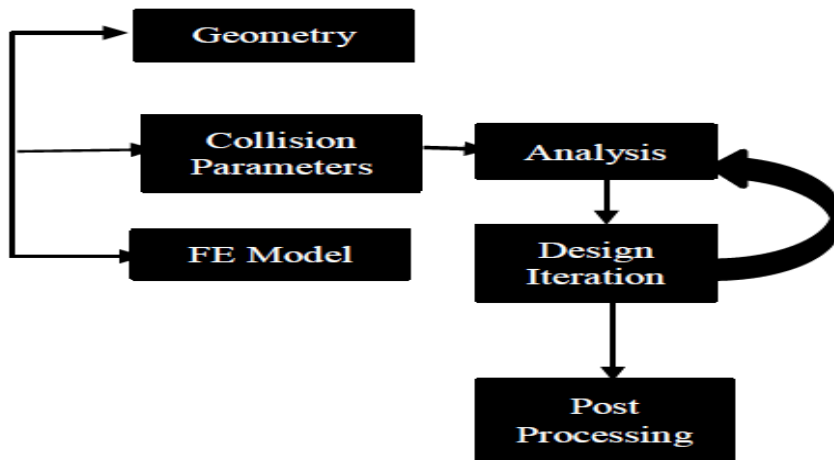
Table 5: Typical Mechanical Properties for S – Glass Fiber / Epoxy (Source: Courtesy of Zweben (1989)).

3.2. Methodology

a) Existing design Study



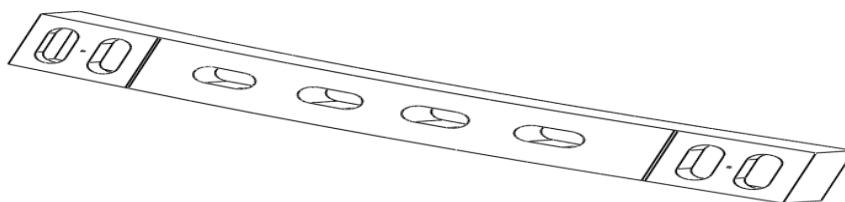
b) Improvement

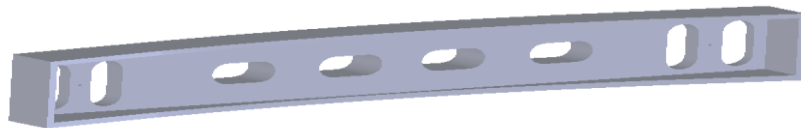
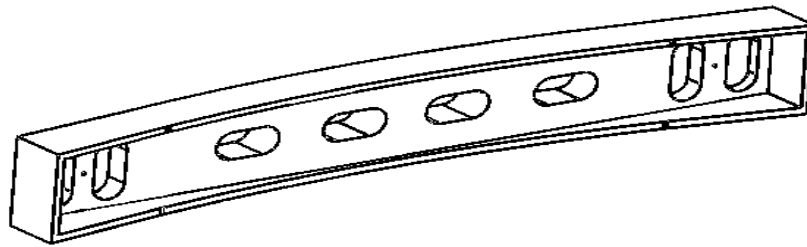


c) Result Validation

The automobile selected for the purpose is **lifan 520** model released in 2011. The bumper of the existing model had steel bumper.

A solidworks model of bumper **beam** of lifan 520 model :





All dimensions are in cm.

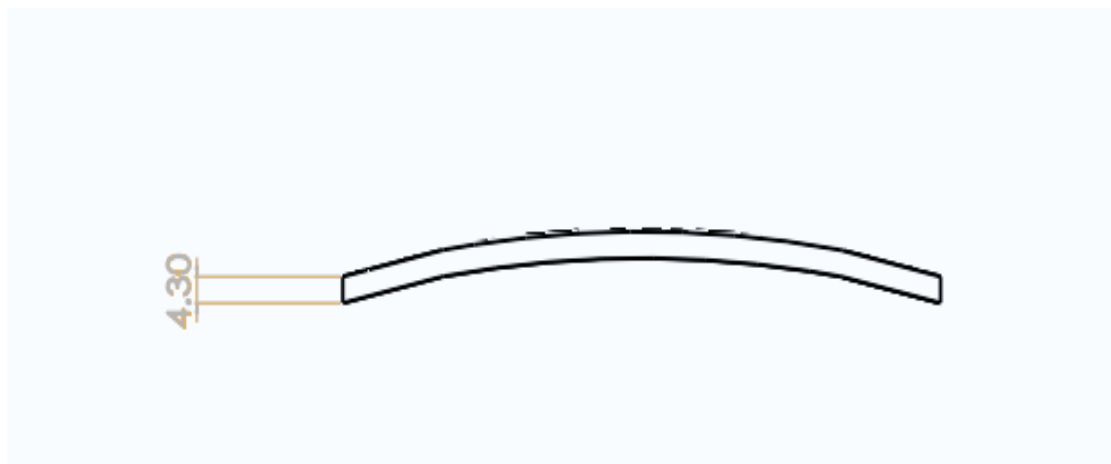
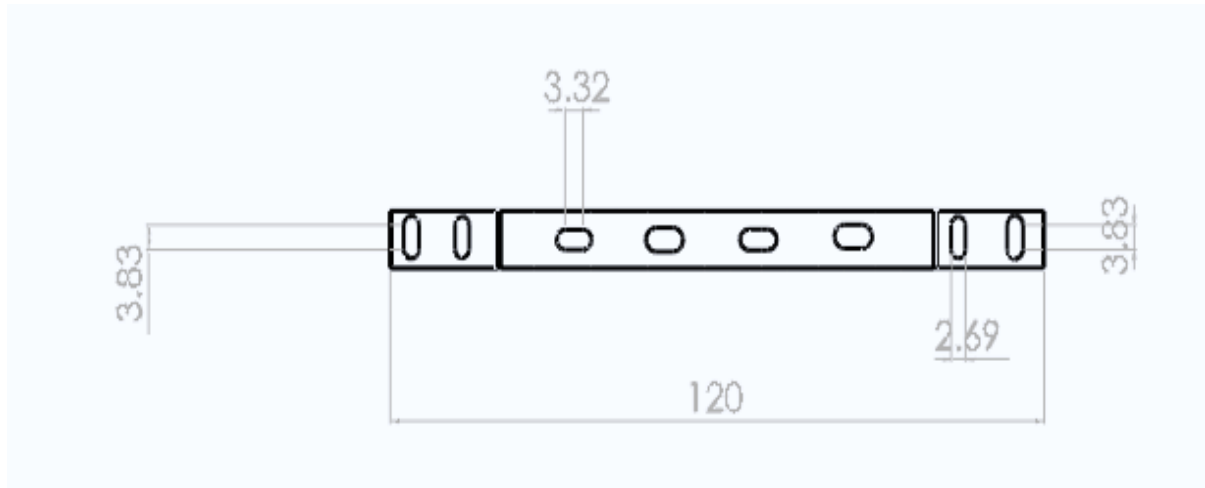


Figure 4: Existing Lifan 520 Model Steel Bumper Beam

3.3. CONDITIONS

3.3.1. Impact condition and tests in automotive structures

With the development of automotive industry, the safety of the car has increasingly become an important research field of modern automobile development design. Also the energy absorption capability of a composite material is important in developing improved human safety in an automotive crash. [29-31]. The ability to absorb impact energy and be survivable for the passengers is called the “crashworthiness” of the structure in vehicle. There are two important safety concepts in automotive industry to consider, crashworthiness, and penetration resistance. [32]. Crashworthiness is defined as the potential of absorption of energy through controlled failure modes and mechanisms that provides a gradual decay in the load profile during allowing projectile or fragment penetration.

The current legislation in design of the automobiles requires that, in the case of impact at speeds up to 15.5m/s (35mph) with a solid, immovable object, the occupants of the passenger compartment should not experience a resulting force that produce a net deceleration greater than 20gm. Subjection of the occupant to decelerations greater than 20 gm can cause serious internal injury, particularly brain damage. [33]

The current trend of materials in car industry is towards replacing metal parts more and more by polymer composites in order to improve the fuel economy and reduce the weight of the vehicles. Also the use of composite materials as energy absorber is important in developing improved human safety in automotive crash. The behavior of composite failure in compression is the opposite of metals. Most composite are generally characterized by a brittle rather than ductile response to load. While metals structures collapse under crush or impact by buckling and/or folding in accordion(concertina) type fashion involving extensive plastic deformation, composite fail through a sequence of fracture mechanisms involving fiber fracture, matrix crazing and cracking, fiber-matrix de-bonding, delamination and interplay separation. The actual mechanisms and sequence of damage are highly dependent on the geometry of the structure, lamina orientation, and type of trigger and crash speed, all of which can be suitably designed to develop high energy absorbing mechanisms. Also the energy absorption in these composite materials is dependent on many parameters such as fiber type, matrix type, fiber architecture, and specimen geometry and fiber volume fraction.

Changes in these parameters can cause subsequent changes in the specific energy absorption (SEA) of composite materials up to a factor of two. [34]

According to the literatures data survey, from different types of impact on automotive car structures, **60.6%** were frontal impacts (that includes car to car impacts and the majority of impact against fixed object and non-motorists), **25.7%** were side impacts (both left and right, and some impacts against fixed objects such as ole), **6.2%** were rear impacts (that include car to car impacts and some impacts against non-motorists). [35]

Vehicle-to-Vehicle Frontal Collisions (types of impact modes)

Vehicle-to-vehicle collisions include many types of impact modes. In this research, only frontal collision is considered. In fact, in most crashes between two vehicles, it is generally the lighter vehicle that is damaged more extensively and whose occupants are subjected to higher loads.

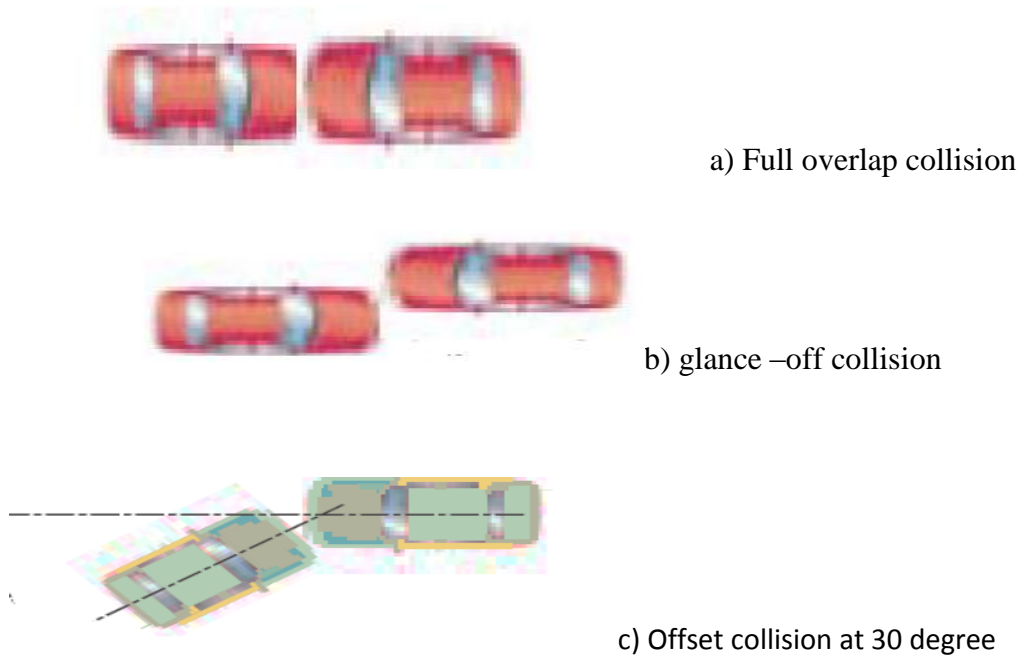


Fig. 4.1. Types of impact modes

Reduction of Biomechanical Injury Values for an Exemplary Sliding collision

Collision type	Edef [MJ]	S [kNs]	$\Delta v1$ [km/h]	$\Delta v2$ [km/h]
Full overlap	1	40,6	58	146
Sliding collision	0,3	9,5	14	34

The fact that injury risk rate of occupants in glance-off is much lower than in full collision is obvious.

3.3.2. Mathematical Model Used for Dynamic Explicit Solution

The basic equations solved by an explicit dynamic analysis express the conservation of mass, momentum and energy in Lagrange coordinates. These, together with a material model and a set of initial and boundary conditions, define the complete solution of the problem. For Lagrange formulations, the mesh moves and distorts with the material it models, so conservation of mass is automatically satisfied. For each time step, these equations are solved explicitly for each element in the model, based on values input at the end of the previous time step. Only mass and momentum conservations are enforced. However, in well-posed explicit simulations, mass, momentum and energy should all be conserved.

DEVELOPMENT OF MATHEMATICAL MODEL FOR THE FRONTAL IMPACT

The simulation result which has been developed has to be validated. But the experimental tests are very expensive and time consuming to do a detailed work on this project. So there are some other ways to validate the model. An alternate way to achieve the proposed result is to develop a numerical model for the bumper and pendulum system for frontal collisions.

The pendulum is modeled simply as a rigid solid of mass M with an initial velocity of V . Otherwise; the car is modeled as a rigid solid of equivalent mass M . However, the stiffness of the bumper beam is included in the model as a spring of stiffness K . This stiffness can be identified either experimentally or analytically. From the mechanics of materials, the stiffness of the beam is $K = 48EI/L^3$ when the external loads applied on its center. Here the E is the Young's modulus of the materials, I is the moment of inertia and L the total length of the bumper beam.

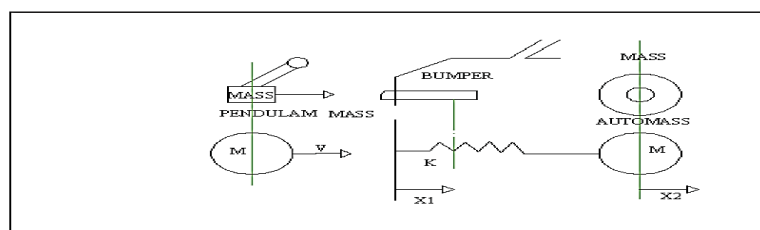


Figure 5: Equivalent spring mass system for bumper and impactor

Since the mass of the bumper is small with respect to the car, it is neglected in this analysis.

However, the stiffness of the bumper is included in the model as a spring of stiffness K_B .

This stiffness can be quantified either experimentally or analytically by considering the displacement 'y' of a bumper beam under a load F from a pendulum. Then the stiffness K_B simply becomes:

$$K_B = \text{LOAD / DEFLECTION} = \frac{F}{y}$$

The governing differential equations for the dynamic system described in Figure:

According to Newton's law of inertia, the generalized inertia load is equivalent to the acceleration multiplied by mass (inertia). Thus, the inertia load distribution has transient (time dependent) characteristics:

The general governing equation of this situation can be formulated from the second order ordinary differential equation of motion.

$$[M]\{\ddot{U}\} + [C]\{\dot{u}\} + [K]\{u\} = \{F\}$$

Where; [M] = structural mass matrix $\{\ddot{u}\}$ = acceleration vector

[C] = structural damping matrix $\{\dot{u}\}$ = velocity vector

[K] = structural stiffness matrix $\{u\}$ = displacement vector

$\{F\}$ = load vector

$$M\ddot{X}_1 + K_B (X_1 - X_2) = 0$$

$$M\ddot{X}_2 + K_B (X_1 - X_2) = 0$$

And the initial conditions are:-

$$X_1(0) = 0$$

$$\dot{X}_1(0) = V$$

$$X_2(0) = 0$$

$$\dot{X}_2(0) = 0$$

The principle of energy conservation in elastic impact is used; the kinetic energy before impact is conserved and converted to elastic energy and the kinetic energy of the impactor and the automobile at its maximum deflection, i.e.,

$$\frac{1}{2}mV_1^2 = \frac{1}{2}K_B[(x_1 - x_2)_{\max}]^2 + \frac{1}{2}mV_2^2 + \frac{1}{2}MV_2^2$$

3.3.3. Load Determination

Estimation of Impact force for a collision

$$\text{Energy Transferred, (kE)} = \frac{1}{2} * \left\{ \frac{(m_1 * m_2)}{(m_1 + m_2)} * (u_2 - u_1)^2 \right\}$$

Where, m_1 and m_2 are the two colliding masses with velocities u_2 and u_1 respectively. Since both m_1 and m_2 are two **vehicles with similar masses** and the vehicle (m_2) is at rest,

$$m_1 = m_2 \quad \& \quad u_2 = 0$$

$$\Rightarrow \text{kE} = \frac{1}{4} * m_1 * \{u_1\}^2$$

Now, Force = kE/t, Where 't' is impact time.

$$\Rightarrow \text{F} = \frac{1}{4} * m_1 * \{u_1\}^2 / t$$

Mass of the vehicle = 1250 Kg (from lifan motors company manual)

Maximum Speed of Vehicle, $u_1 = 48 \text{ km/hr.} = 13.3 \text{ m/s}$ (moderate vehicle speed) This speed is according to regulations of Federal Motor Vehicle Safety Standards, FMVSS 208-Occupant Crash Protection whereby the purpose and scope of this standard specifies requirements to afford impact protection for passengers. [36, 37]

In most crash time t is of the order of 0.1s.

$$\Rightarrow \text{F} = \frac{1}{4} * 1250 * \{13.3\}^2 / 0.1 = 312 \text{ KN.}$$

The Design Factor of Safety, FSD was taken as 1.5. This relatively high value is taken to account for the uncertainty in the nature of forces.

$$\Rightarrow \text{F} = 1.5 * 312 = 468 \text{ KN.}$$

Hence for design purposes force is taken to be 468 KN.

For the easiness of calculation this force is converted into a pressure which is acted on the front surface of the modelled bumper.

Area of the front face of bumper beam $=l*b = 0.11184 \text{ m}^2$

l = length of front face in mm, b = breadth of front face in mm

Pressure acted on the bumper $= F/A = 468000/0.18130187 = 2581330 \text{ N/m}^2 = 2.5 \text{ MPa}$

F = Force acted during collision in Newton's, A = Area of the front face of bumper in m^2 .

CHAPTER FOUR

FINITE ELEMENT IMPACT SIMULATION USING ANSYS SOFTWARE

Finite Element Analysis

Simulation using finite element method comprises of three major phases:

- Pre-processing, in which the analyst develops a finite element mesh to divide the subject geometry into sub domains for mathematical analysis, and applies material properties and boundary conditions,
- Solution, during which the program derives the governing matrix equations from the model and solves for the primary quantities, and
- Post-processing, in which the analyst checks the validity of the solution, examines the values of primary quantities (such as displacements and stresses), and derives and examines additional quantities (such as specialized stresses and error indicators).

4.1. Existing Lifan 520 Model Bumper

The bumper beam over all thickness is 5 mm.

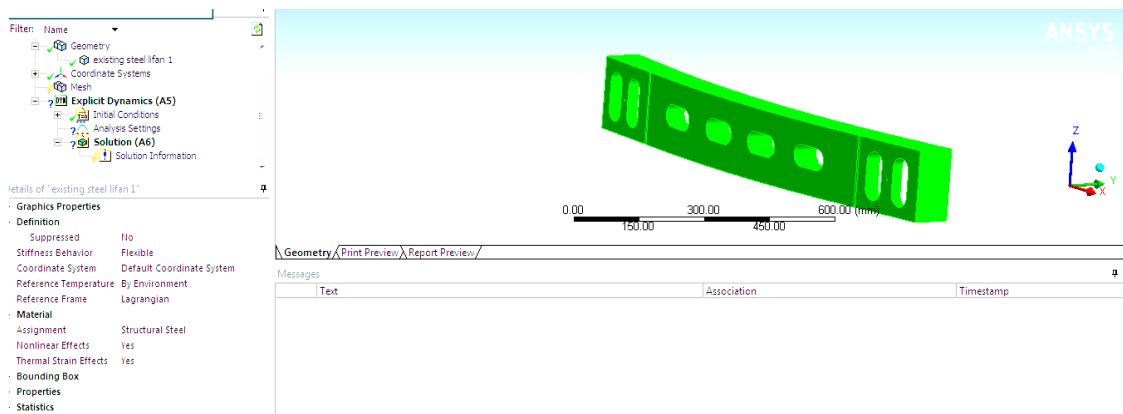


Figure 6: Existing Lifan 520 Model Bumper

4.1.1. Meshing

Once all of this information is assembled in to an FEA model, the analyst can begin with a preliminary mesh. Early in the analysis process, it makes sense to start with a mesh that is as coarse as possible –a mesh with very large elements. A coarse mesh will require less computational resources to solve and, while it may give a very inaccurate solution, it can still

be used as a rough verification and as a check on the applied loads and constraints. After computing the solution on the coarse mesh, the process of mesh refinement begins. In its simplest form, mesh refinement is the process of resolving the model with successively finer and finer meshes. This comparison can be done by analyzing the fields at one or points in the model or by evaluating the integral of field over some domains and boundaries. by comparing these scalar quantities, it is possible to judge the convergence of the solution with respect to mesh refinement.

The average thickness of impact beams are smaller than the other dimension of the part, the best meshing for the element was the shell element with the type of three node-triangular elements. The imported geometry is meshed with smooth grid elements which give the number of elements as 5405 and number of nodes as 16594.

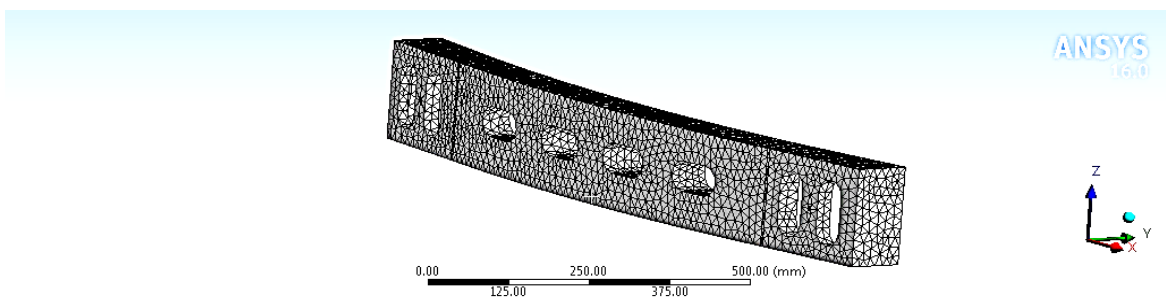


Figure 7: Meshing

4.1.2. Fixed Support

A fixed support which is from the boundary condition i.e. One car is moving and the other is at rest. A fixed support is placed where a car bumper beam is mounted on a vehicle body position.

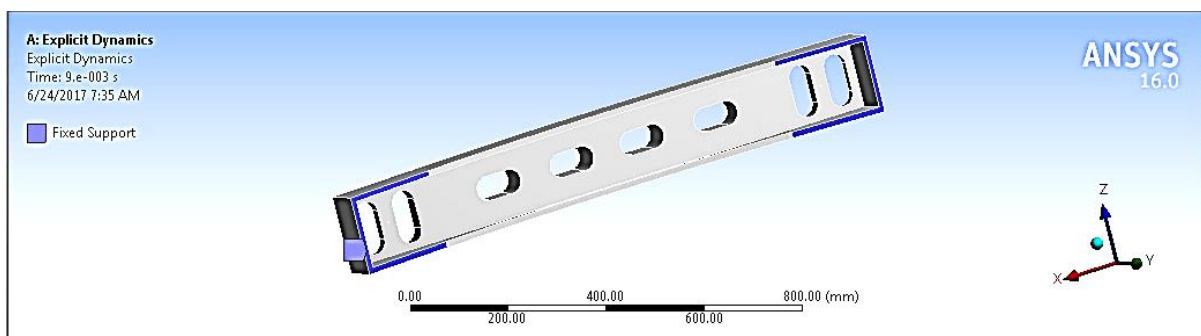


Figure 8: Fixed Support

4.1.3. Impact Load

Here the impact force applied by the moving car is not a point load so it should convert to a pressure load to frontal surface of the bumper beam.

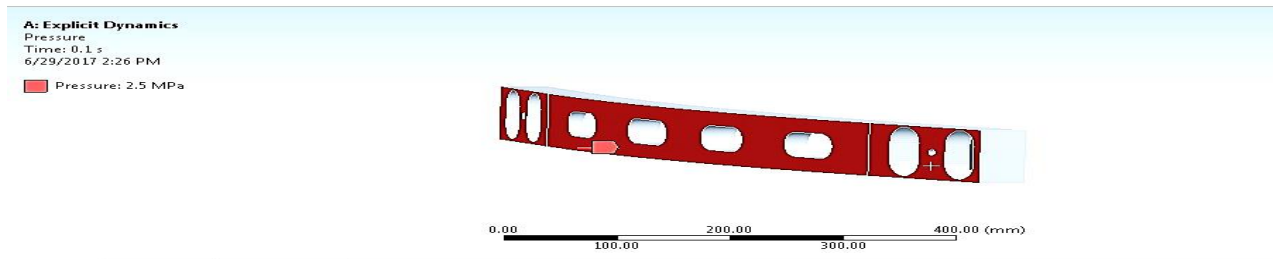


Figure 9: Impact Load

4.2. Modified S –Glass Fiber Reinforced Epoxy Bumper Beam

The thickness and the geometry have changed to 4 mm and solid surface respectively. Reduction of thickness is to get light weight bumper beam and the solid surface can add some strength and reduce stress concentration during impact.

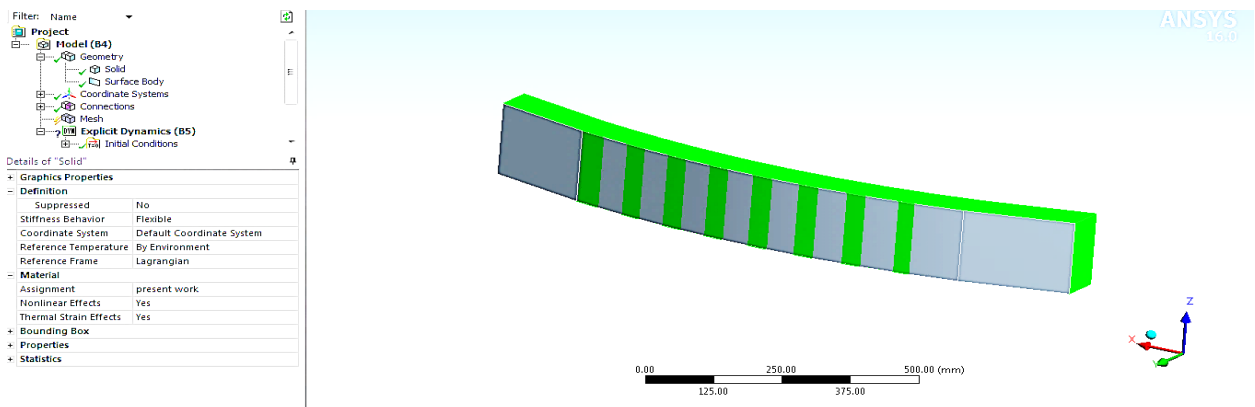


Figure 10: Optimized S –Glass Fiber Reinforced Epoxy Bumper Beam

4.2.1. Layered Section

Before layers are set in the worksheet to the face surface as shown below

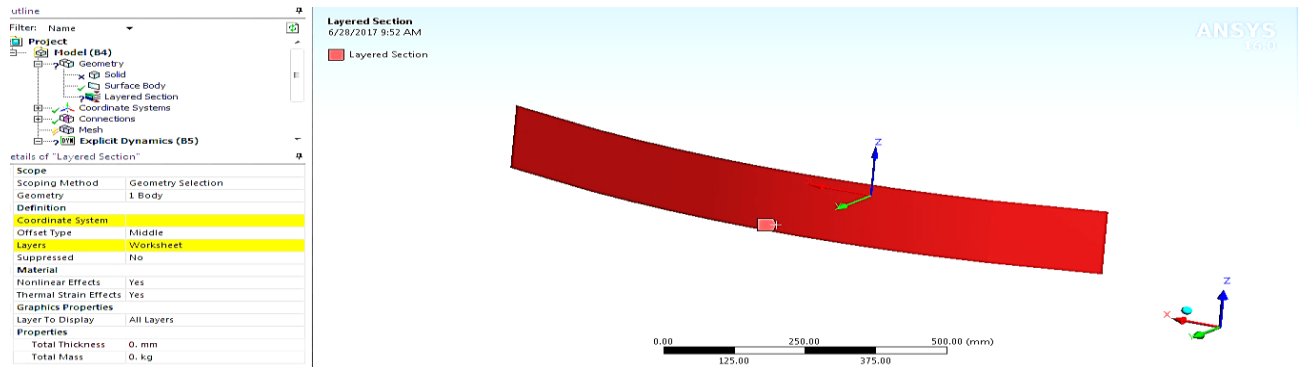


Figure 11: Face Surface of the Beam

And here 8 layers are set with different fiber orientation as shown below, 0.5 mm thickness because a total thickness of 4 mm.

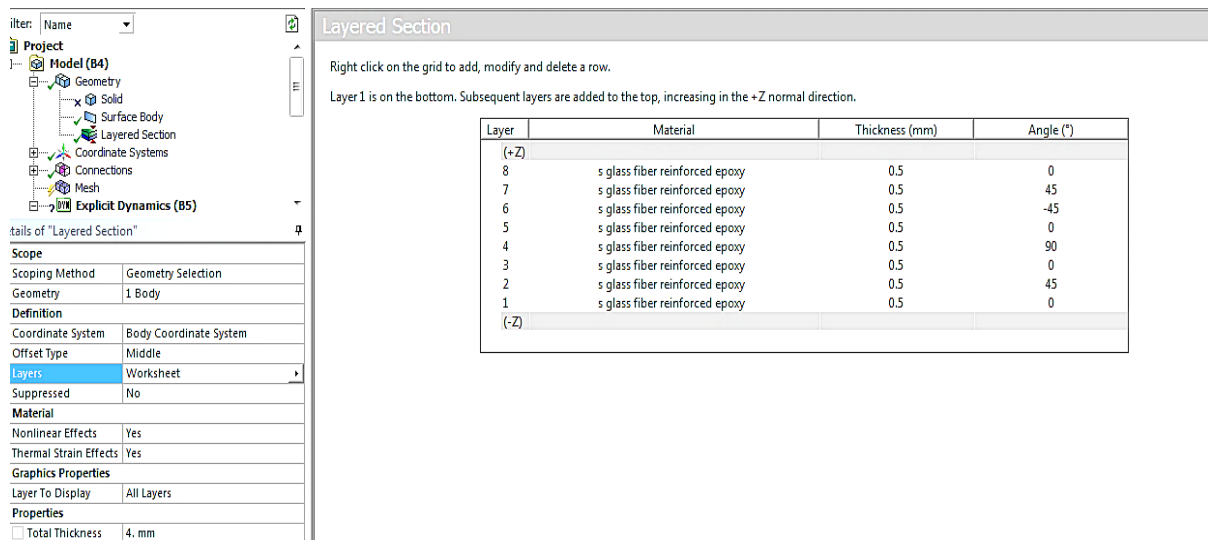


Figure 12: Layered Section

4.2.2. Meshing

Due to those layers the surface body with 0.5 mm thickness becomes a 4 mm thick surface. The average thickness of impact beams are smaller than the other dimension of the part, the best meshing for the element was the shell element with the type of four node-rectangular elements. The imported geometry is meshed with smooth grid elements which give the number of elements as 424 and number of nodes as 810.

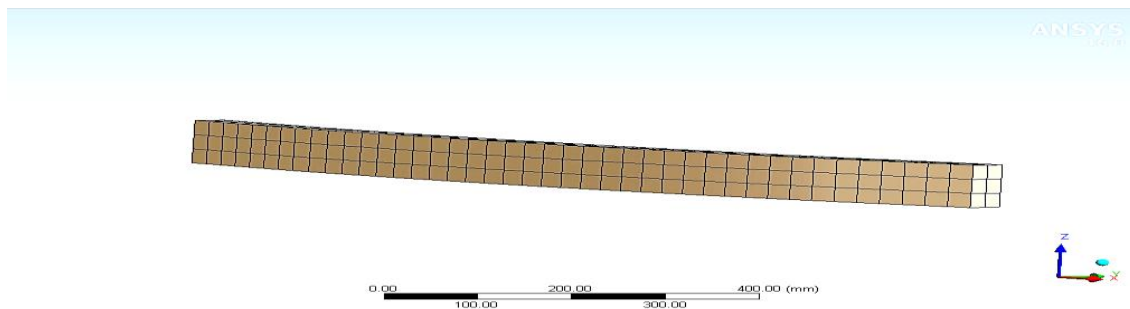


Figure 13: Meshing of S Glass Fiber Reinforced Epoxy Beam Material

CHAPTER FIVE

RESULT AND DISCUSSION

5.1. Existing AISI 1006 Steel Bumper Beam Results

5.1.1. Total Deformation

Due to the applied pressure load maximum deformation length is 4.8 mm as shown in the graph. But 4.1619 mm is total deformation.

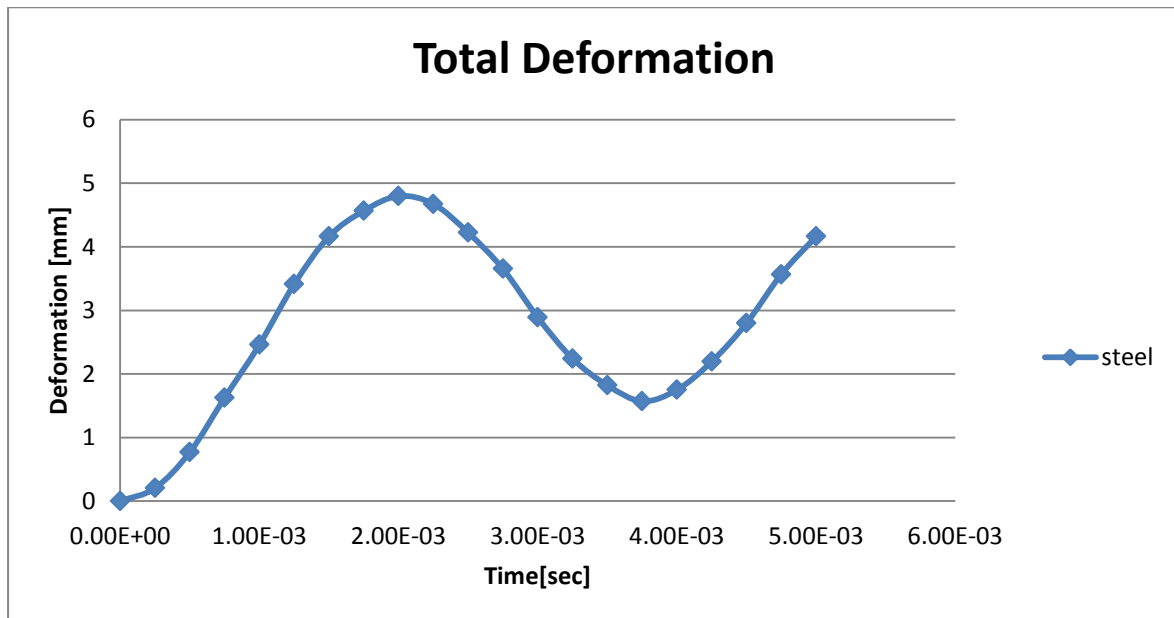
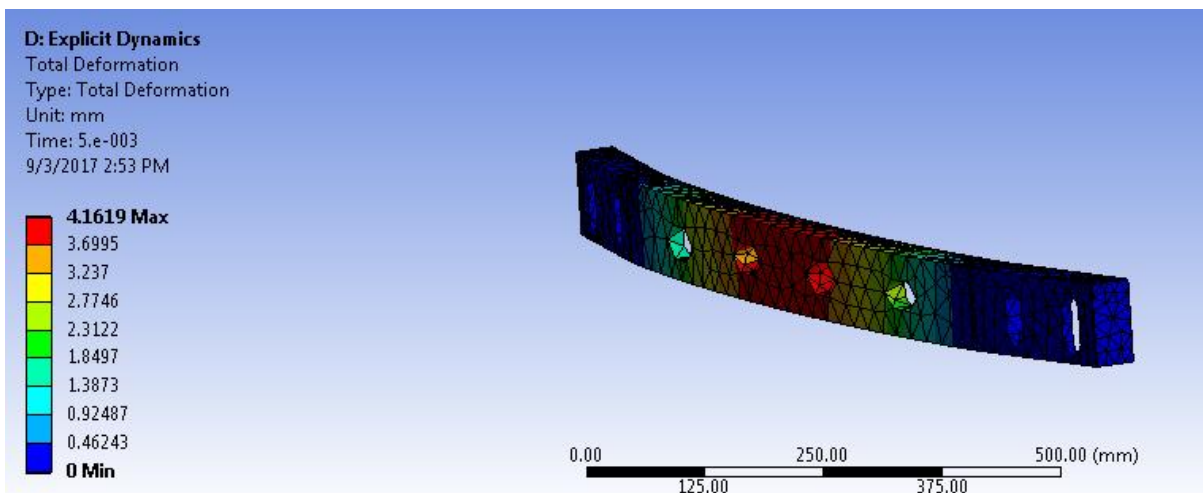


Figure 14: Total Deformation of Steel Bumper Beam

5.1.2. Equivalent Elastic Strain

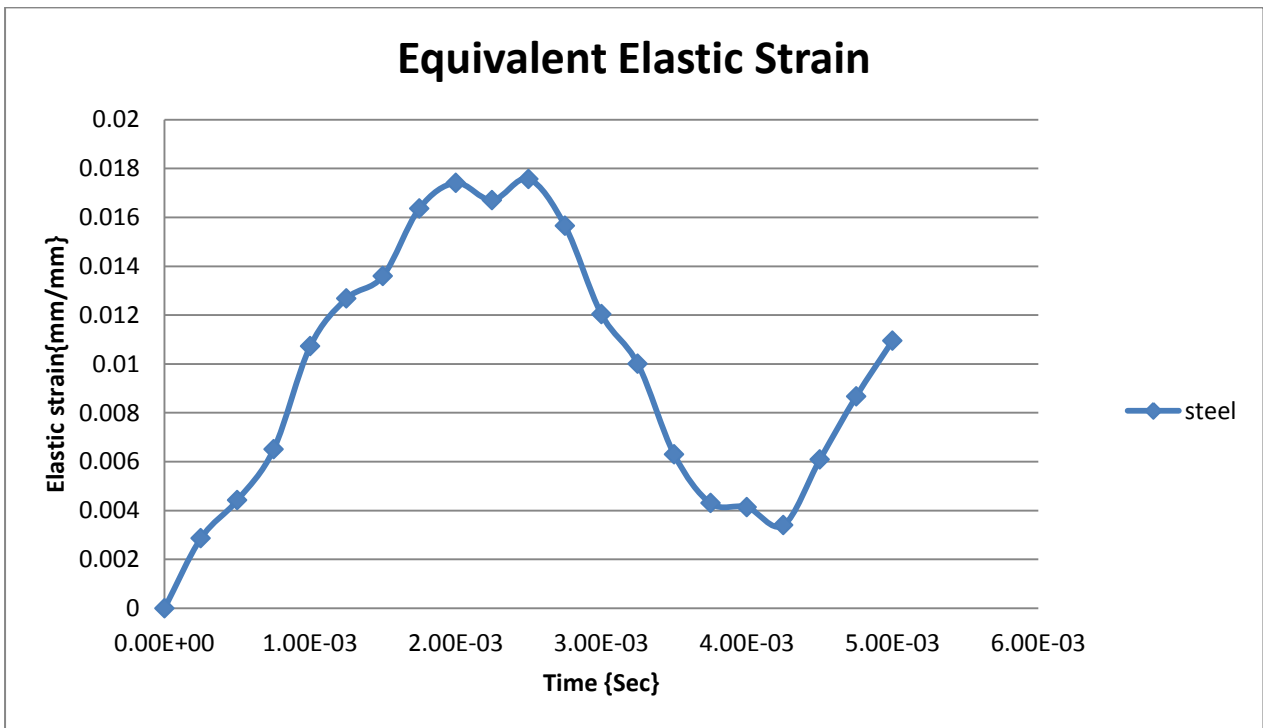
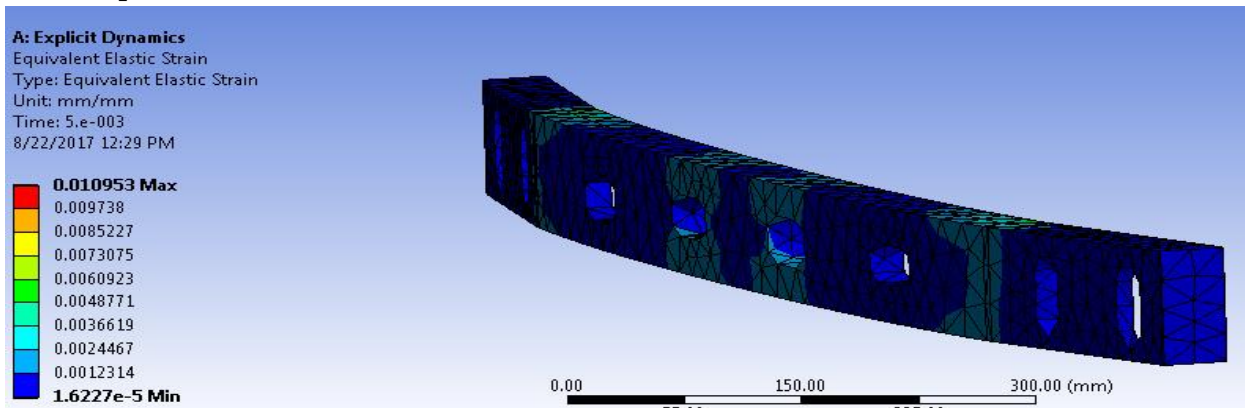


Figure 15: Equivalent Elastic Strain

5.1.3. Equivalent (von –mises) stress

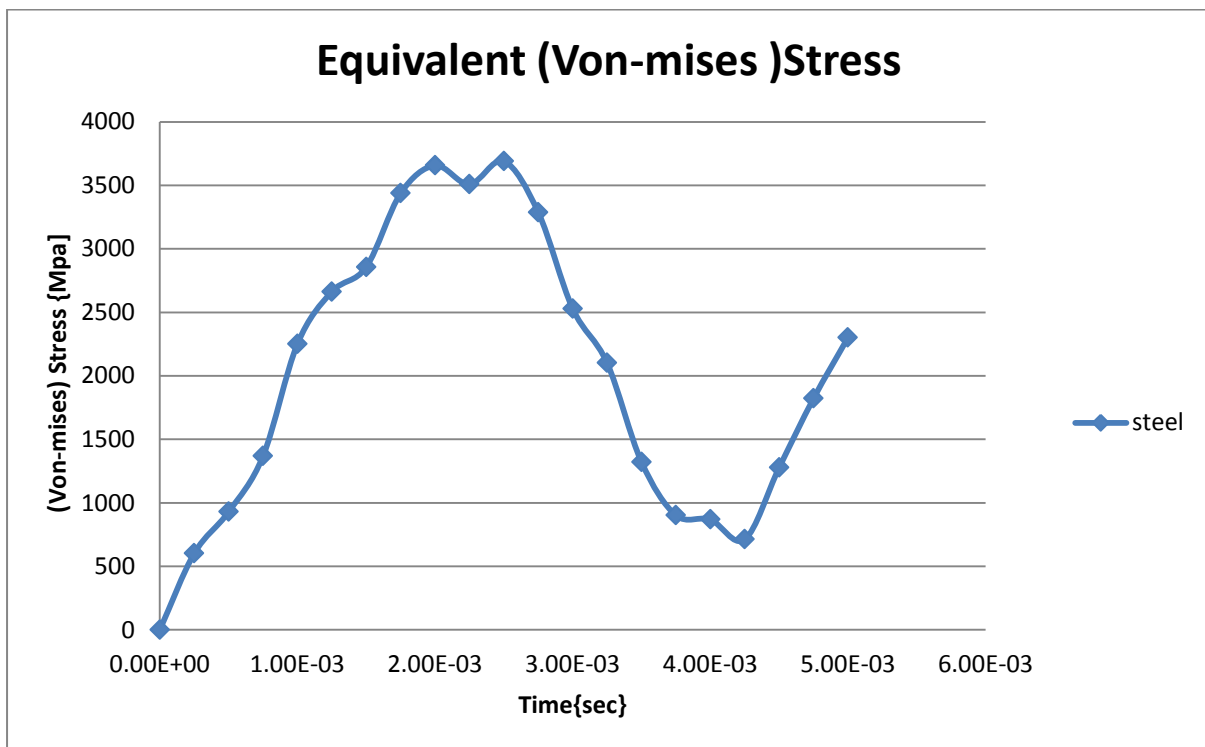
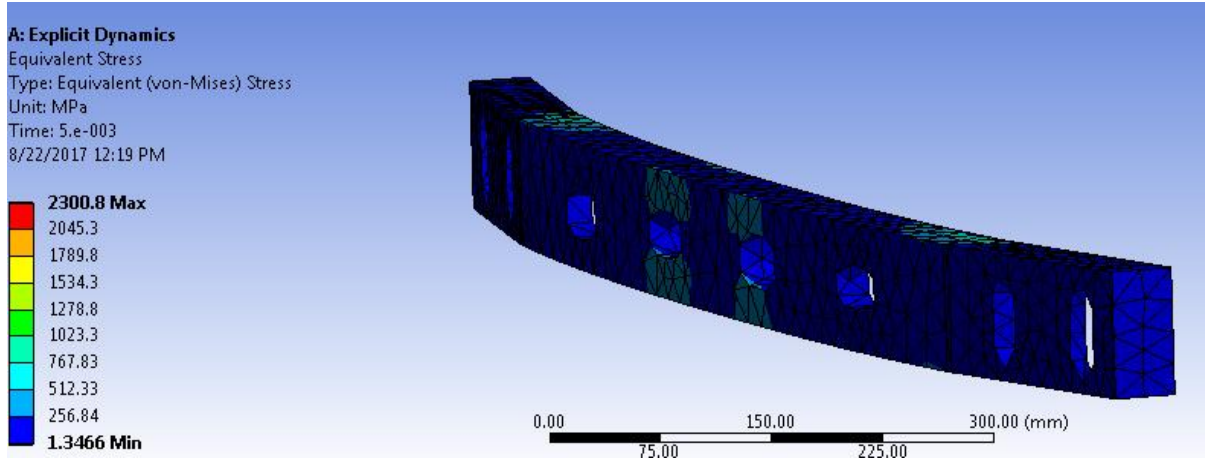


Figure 16: Equivalent (Von-Mises) Stress

5.1.4. Internal Energy

Which is the energy absorbed by the 1006 steel beam material

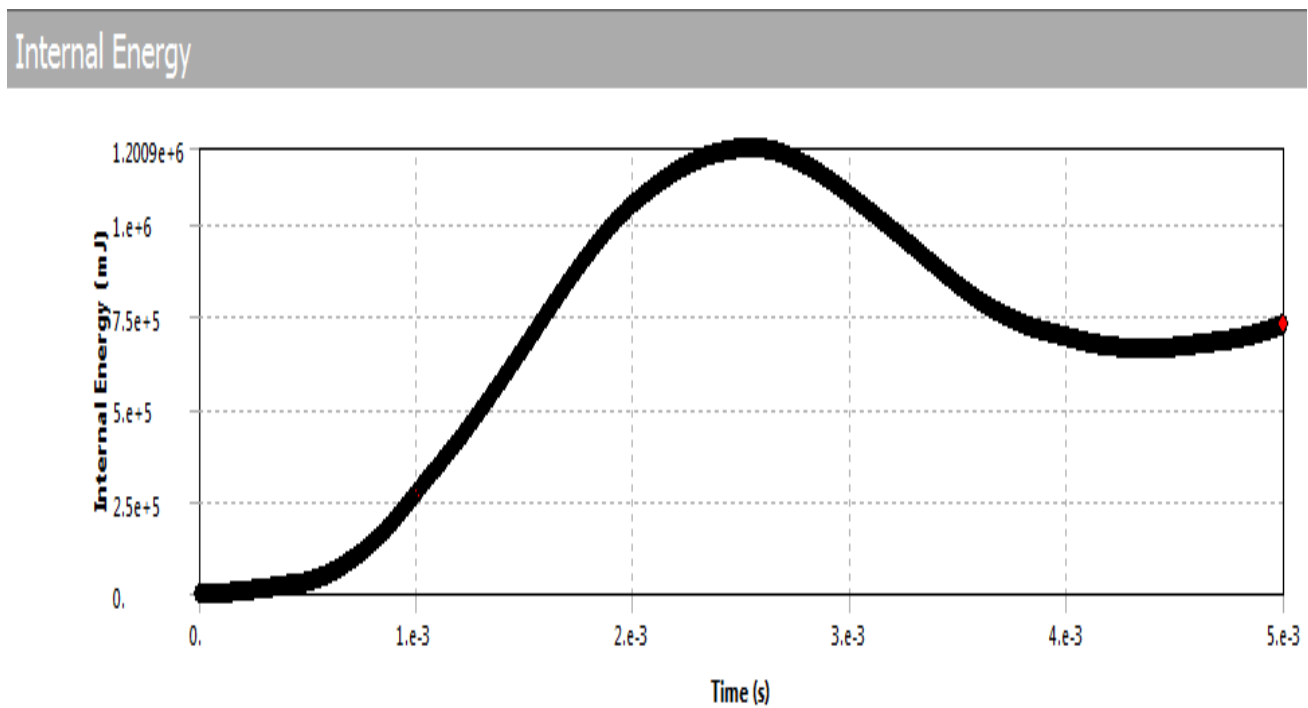
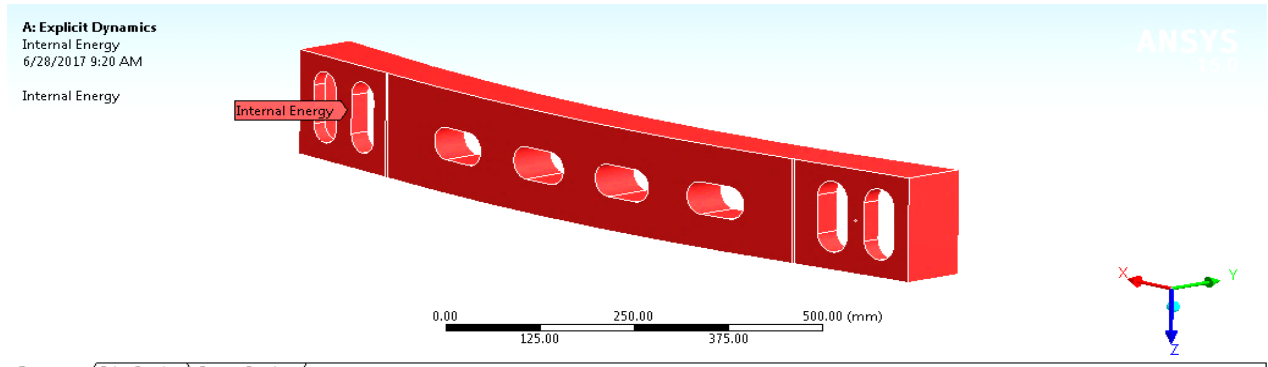


Figure 17: Internal Energy

In theory, internal energy is equal to the work (E) done by external forces on the system, which is equal to the product of the exerted force (F) and the distance (d) through which the force moves:

$$E=F.d$$

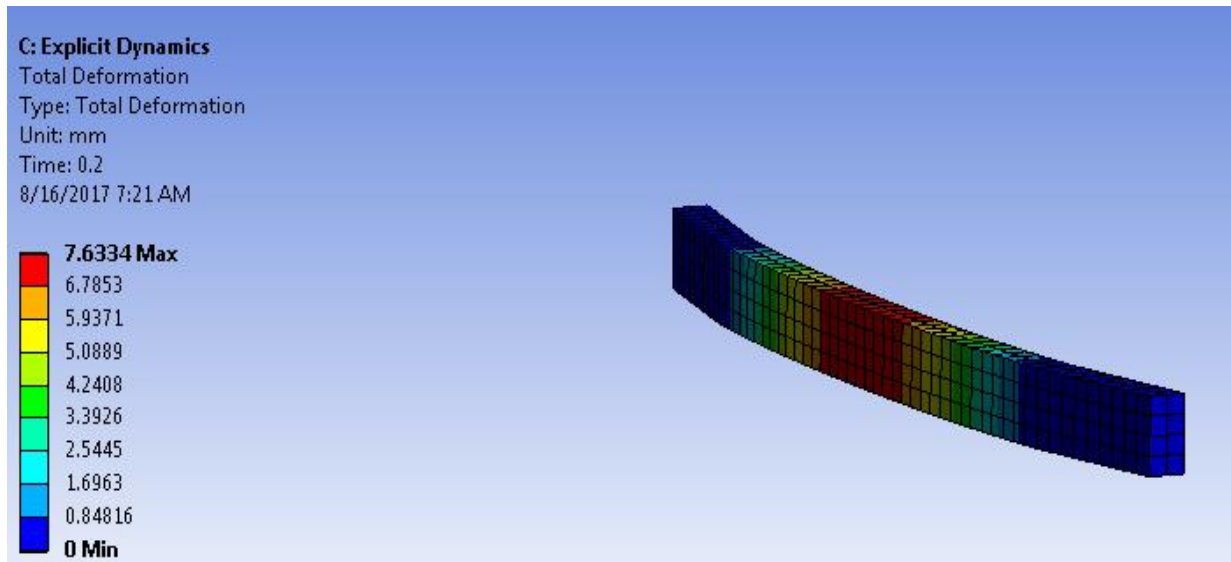
But the load is pressure load which is 2.5 Mpa and it is applied on the front face of bumper beam and due to this load the steel or existing lifan 520 model bumper beam has maximum deflection of 4.8 mm.

However from the above internal energy graph, steel bumper beam absorbs 1.2009×10^6 mJ. This is equals to $(1.2009 \times 1000000) / 1000 = 1200.9$ J

5.2. Modified s glass fiber reinforced epoxy composite bumper beam

5.2.1. Total Deformation

Due to the applied pressure load maximum deformation length is 1.84 mm as shown in the graph. But 7.6334 mm as a total deformation at $t=0.2$ sec.



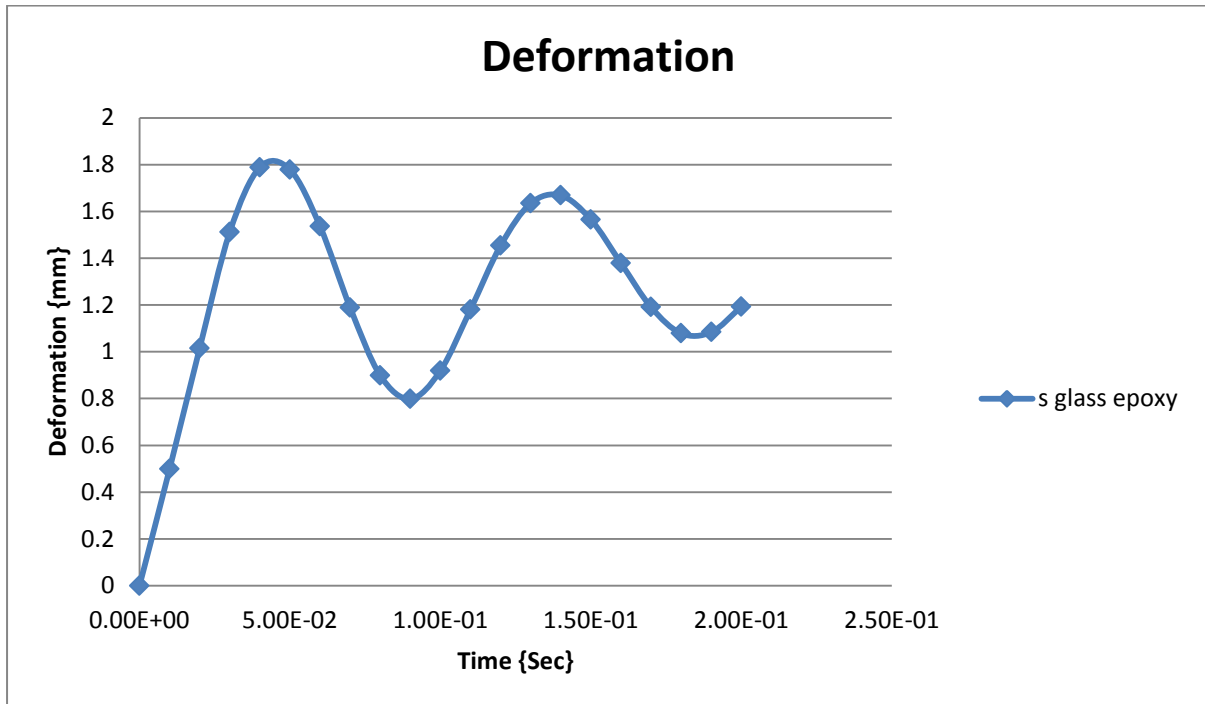
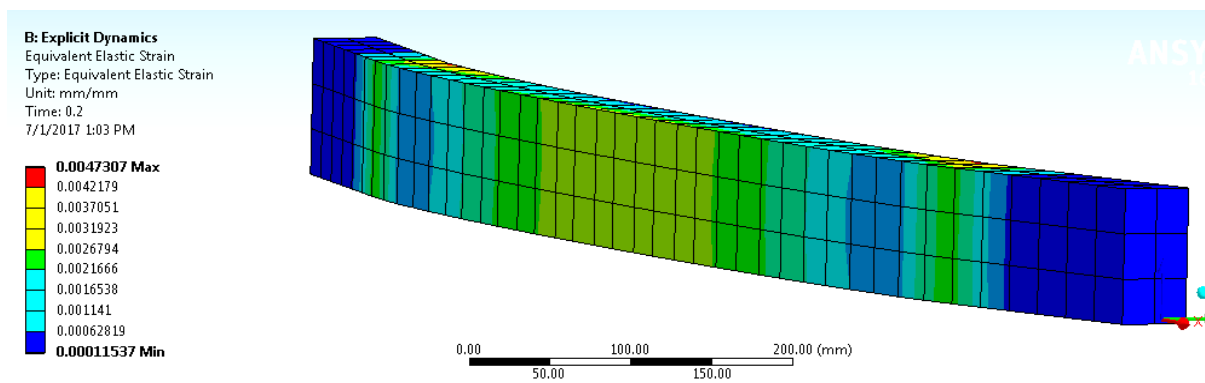


Figure 18: Total Deformation of S Glass Fiber Reinforced Epoxy Beam Material

5.2.2. Equivalent Elastic Strain



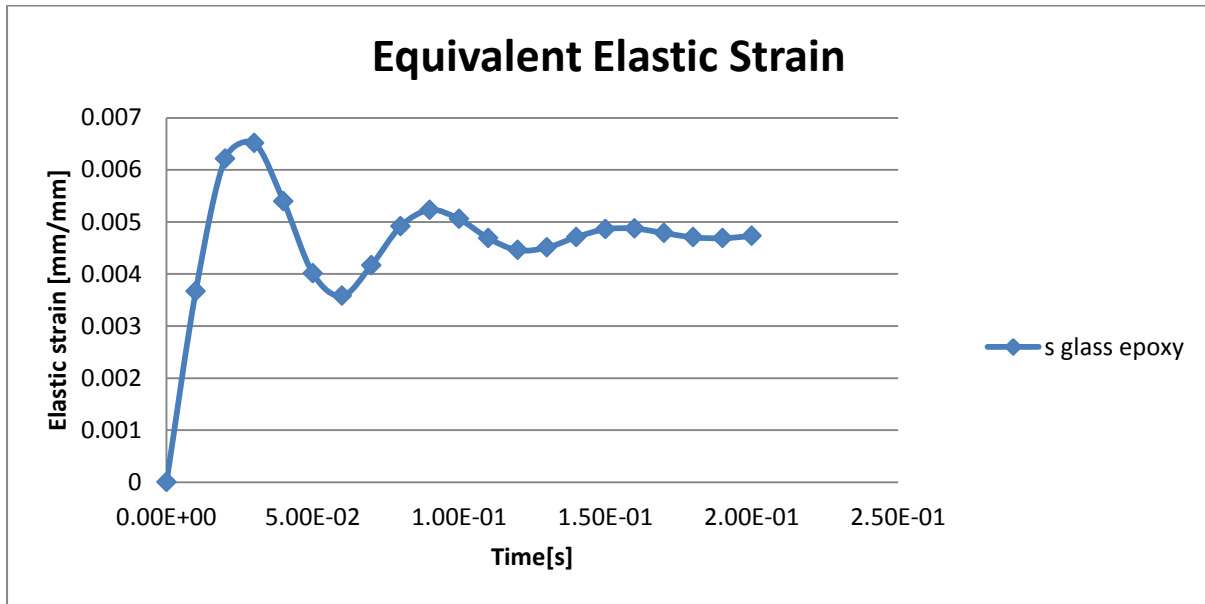
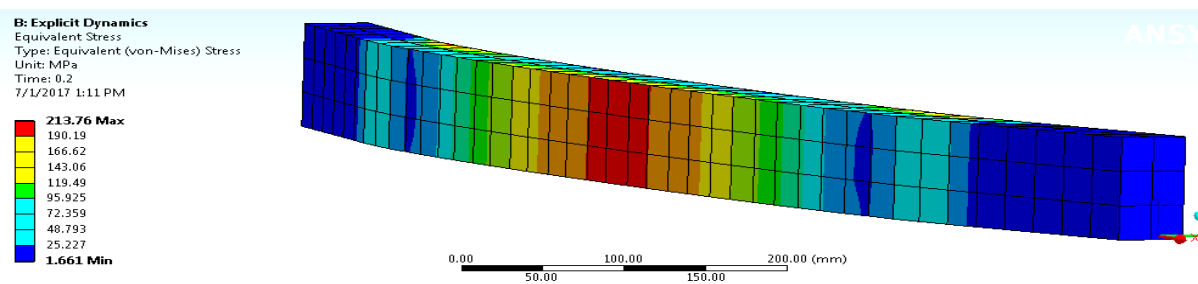


Figure 19: Equivalent Elastic Strain

5.2.3. Equivalent (Von-Mises) Stress



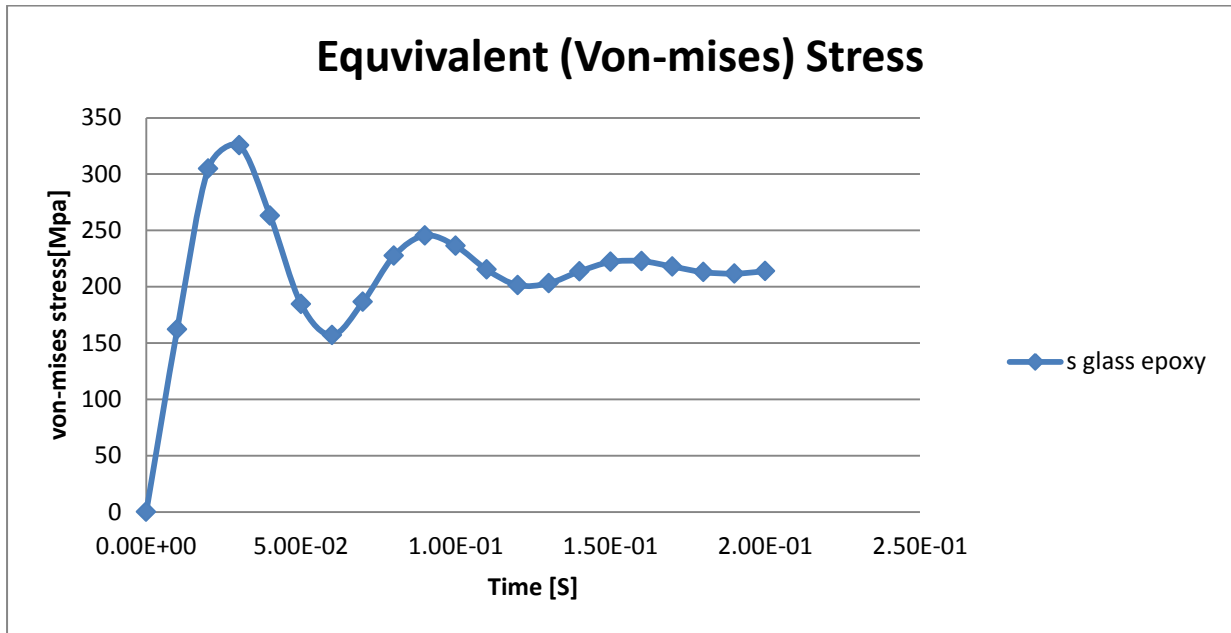


Figure 20: Equivalent (Von-Mises) Stress

5.2.4. Internal Energy

Which is the energy absorbed by the s-glass fiber reinforced epoxy material

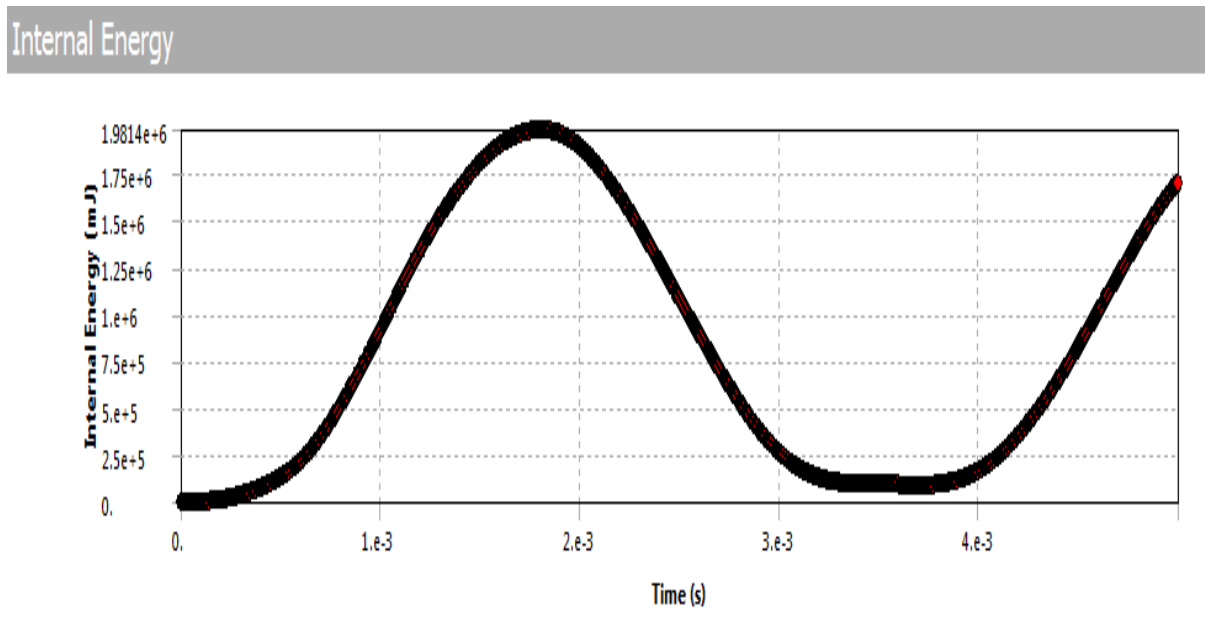


Figure 21: Internal Energy

In theory, internal energy is equal to the work (E) done by external forces on the system, which is equal to the product of the exerted force (F) and the distance (d) through which the force moves:

$$E=F.d$$

But the load is pressure load which is 2.5 Mpa and it is applied on the front face of bumper beam and due to this load the s glass fiber reinforced epoxy bumper beam has an elastic deformation 1.84mm.

However from the above internal energy graph, s glass fiber reinforced epoxy composite absorbs 1.98×10^6 mJ. This is equals to $(1.98 \times 1000000)/1000 = 1980$ J

5.3. Result and discussion

5.3.1. Total deformation

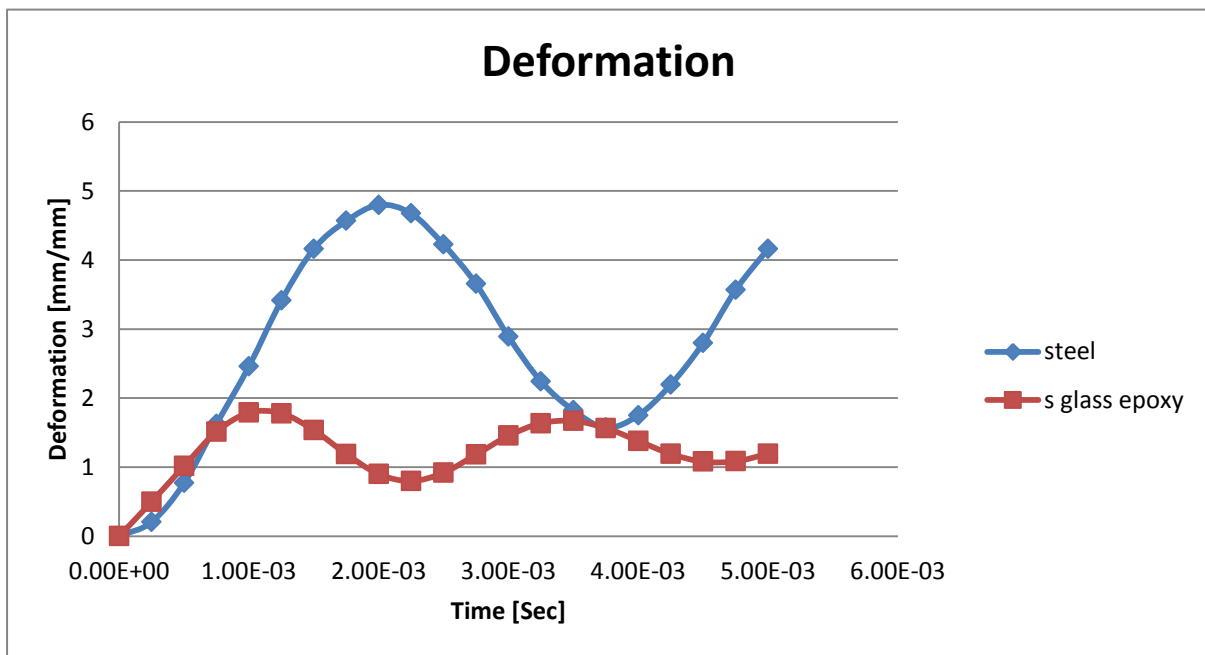


Figure 22: Total Deformation of Both Materials

5.3.2. Equivalent Elastic Strain

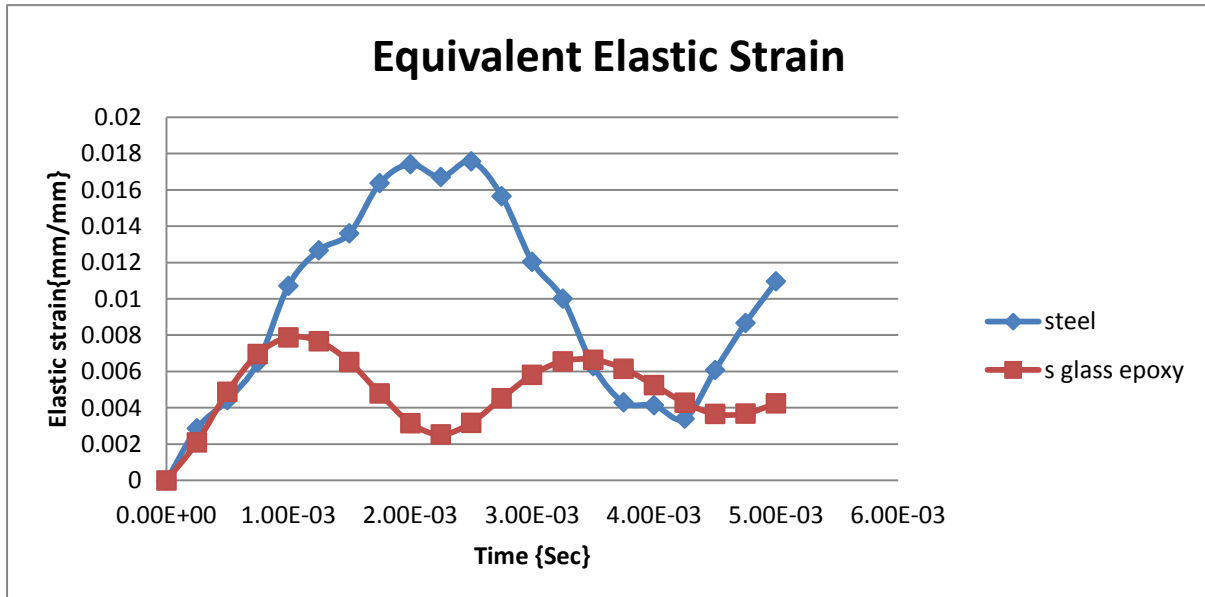


Figure 23: Equivalent Elastic Strain of Both Materials

5.3.4. Internal Energy

In theory, internal energy is equal to the work (E) done by external forces on the system, which is equal to the product of the exerted force (F) and the distance (d) through which the force moves:

$$E = F \cdot d$$

But the load is pressure load which is 2.5 Mpa and it is applied on the front face of bumper beam and due to this load the structural steel or existing lifan 520 model bumper beam has an elastic deformation of 11mm.

However from the above internal energy graph, steel bumper beam absorbs $1.2009 \cdot 10^6$ mJ. This is equals to $(1.2009 \cdot 1000000) / 1000 = 1200.9$ J

And also the load is pressure load which is 2.5 Mpa and it is applied on the front face of bumper beam and due to this load the s glass fiber reinforced epoxy bumper beam has an elastic deformation of 1.84 mm.

However from the above internal energy graph, s glass fiber reinforced epoxy composite absorbs $1.98 \cdot 10^6$. This is equals to $(1.98 \cdot 1000000) / 1000 = 1980$ J

CHAPTER SIX

CONCLUSION AND RECOMMENDATION

6.1. CONCLUSION

Bumper beam is an important member of an automobile from the safety point of view. Thus the analysis of bumper will help to increase the safety of passengers and new size, shape and material may also be considered to replace the existing one. Design of composite bumper (using s glass fiber material) is completed and also composite bumper is analyzed and compared with steel bumper.

- The steel bumper has a deformation of 4.8 mm where the composite bumper beam has a deformation of 1.84 mm which is 61.6% high strength than steel bumper.
- The internal energy which is absorbed by steel material is 1200.9 J where the composite material is 1980 J which is 39 % higher than that of steel.
- The existing and composite bumper is analyzed in ANSYS16.0 and the Maximum stress induced in the composite bumper is 213.76 Mpa where steel is 2300.3 Mpa.

From the study, it is concluded that s glass fiber reinforced epoxy composite has better energy absorption capacity than steel material and fiber reinforced plastic material is a suitable material for manufacturing the bumper.

6.2. RECOMMENDATION

The following recommendations for future work can be noted:

- Impact analysis of woven or cross-ply laminated glass/epoxy composite laminate or by using different natural fiber composites in order to improve the energy absorption capacity during transverse impact.
- It is better to do with hybrid materials, glass fibers with natural fibers to optimize better energy absorption.
- ABAQUS software is better for composite materials analysis than ANSYS workbench.
- It is better making the two colliding cars in motion to get better result.
- Finding material properties are very difficult .so characterization is better in the material laboratory.

REFERENCES

1. **Witteaman WJ**, “Improved Vehicle Crashworthiness Design by Control of the Energy Absorption for Different Collision Situations”, Doctoral dissertation, Eindhoven University of Technology, 2000.
2. **D.M. Miller**, Glass Fibers, Composites, Vol 1, Engineered Materials Handbook, ASM International, 1987, p 45-48.
3. **Marzbanrad JM, Alijanpour M, and Kiasat MS**, “Design and analysis of automotive bumper beam in low speed frontal crashesh”, Thin Walled Struct., 47 (2009): 902- 911.
4. **Heinz Heisler**, "Advanced Vehicle Technology", 2nd Ed., Butterworth Heinemann, 2002.
5. **J.F. Dockum, Jr.**, Fiberglass, in Handbook of Reinforcement for Plastics, J.V. Milewski and H.S. Katz, Ed., Van Nostrand Reinhold Company, New York, 1987, p 233-286.
6. **Hosseinzadeh RM, Shokrieh M, and Lessard LB**, “Parametric study of automotive composite bumper beams subjected to low-velocity impacts”, J. Composite Stuct., 68 (2005):419-427.
7. **Marzbanrad JM, Alijanpour M, and Kiasat MS**, “Design and analysis of automotive bumper beam in low speed frontal crashesh”, Thin Walled Struct., 47 (2009): 902- 911.
8. [http://www.nhtsa.dot.gov/cars/testing/procedures/TP- 581-01.pdf](http://www.nhtsa.dot.gov/cars/testing/procedures/TP-581-01.pdf).
9. **Mohapatra S**, “Rapid Design Solutions for Automotive Bumper Energy Absorbers using Morphing Technique”, Altair CAE users Conference 2005, Bangalore, India.
10. http://www.google.com/patents/about/6817638_Bumper_system.html?id=c1gQAAAAEBAJ
11. **Andersson R, Schedin E, Magnusson C, Ocklund J**, “The Applicability of Stainless Steel for Crash Absorbing Components”, SAE Technical Paper, 2002.
12. **Butler M, Wycech J, Parfitt J, and Tan E**, “Using Terocore Brand Structural Foam to Improve Bumper Beam Design”, SAE Technical Paper, 2002,

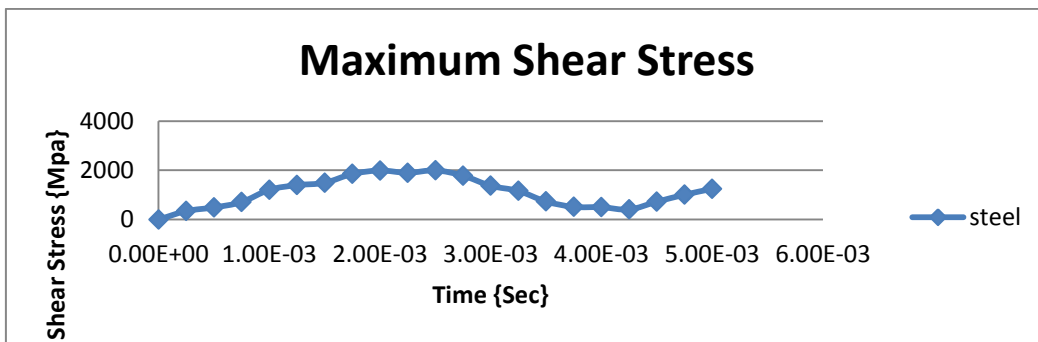
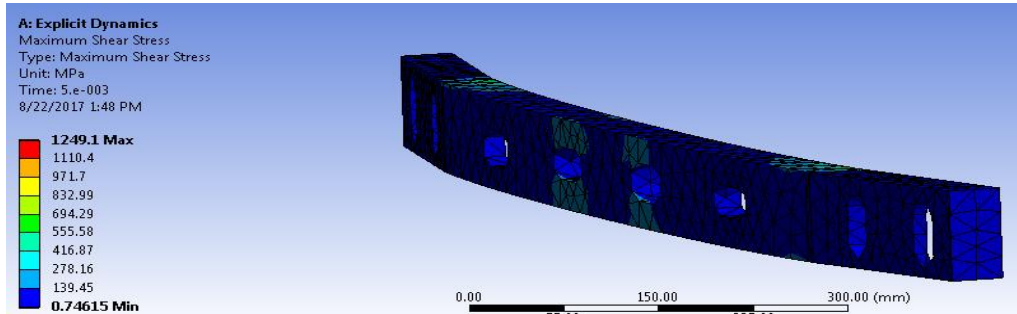
-
- 13. Carley ME, Sharma AK, Mallela V**, “Advancements in expanded polypropylene foam energy management for bumper systems”, SAE Technical Paper, 2004.
- 14. Evans D and Morgan T**, “Engineering Thermoplastic Energy for Bumpers”, SAE Paper, 1999.
- 15. Witteman WJ**, “Improved Vehicle Crashworthiness Design by Control of the Energy Absorption for Different Collision Situations”, Doctoral dissertation, Eindhoven University of Technology, 2000.
- 16. Zonghua Zhang, Shutian Liu, Zhiliang Tang**, “Design optimization of cross-sectional configuration of ribreinforced thin-walled beam” Dalian University of Technology, Dalian, China. 2009. PP 868–878.
- 17. O. G. Lademo, T. Berstad, M. Eriksson, T. Tryland, T. Furuc, O. S. Hopperstad, M. Langseth**, “A model for process-based crash simulation” Norwegian University of Science and Technology Trondheim, Norway 2008.PP. 376–388.
- 18. Nitin S. Gokhale, Sanjay S. Deshpande, Dr. Anand N. Thite**, "Practical Finite Element Analysis", Finite to Infinite, India, 2007.
- 19. Gupta N, Balrajsinghbrar and Eyassuwoldesenbet**. Effect of filler addition on the compressive and impact properties of glass fiber reinforced epoxy. Bull Mater Sci 2001; 24: 219–223.
- 20. Faizal MA, Beng YK and Dalimin MN**. Tensile property of hand lay-up plain-weave woven e glass/polyester composite: curing pressure and ply arrangement effect. Borneo Sci 2006; 19: 27–34. 9. Leonard LWH, Wong KJ,
- 21. Hussain Al-alkawi J, Dhafir Al-Fattal S and Abdul-Jabar Ali H**. Fatigue behavior of woven glass fiber reinforced polyester under variable temperature. Elixir mech Eng 2012; 53: 12045–12050.
- 22. Sapuan, S.M., Maleque, M.A., Hameedullah, M., Suddin, M.N. and Ismail, N.** 2004, A note on the conceptual design of polymeric composite automotive bumper system, J. Mater. Production Tech, Vol.159, pp.145-151.

-
- 23. P.F. Aubourg and W.W. Wolf**, "Glass Fibers- Glass Composition Research," presented at Glass Division Meeting (Grossinger, NY), American Ceramic Society, Oct 1984
- 24. K.L. Loewe; stein**, The Manufacturing Technology of Continuous Glass Fibers, 3rd revised ed., Elsevier, 1993
- 25. D.M. Miller, Glass Fibers**, Composites, Vol 1, Engineered Materials Handbook, ASM International, 1987, p 45-48
- 26. J.F. Dockum, Jr., Fiberglass**, in Handbook of Reinforcement for Plastics, J.V. Milewski and H.S. Katz, Ed., Van Nostrand Reinhold Company, New York, 1987, p 233-286
- 27. ACI Committee 440, Farmington Hills** Report on fiber-reinforced polymer (FRP) reinforcement for concrete structures. MI. 2007.
- 28. J. L. Clarke. London: Blackie** Academic & Professional Glass fiber reinforcing bars. In Alternative materials for the reinforcement and prestressing of concrete, ed. 1993
- 29. Pradeep Kumar Uddandapu:** ‘ Impact analysis on car Bumper by varying speeds using materials ABS plastic and poly Ether Imide by Finite Element Analysis software Solid Works’, International Journal of Modern Engineering Research(IJMER), Vol.3,Jan-Feb 2013,pp. 391-395.
- 30. Haining Chen, Hao Chen, Liangjie Wang:** ‘Analysis of vehicle seat and research on structure optimization in front and rear impact’, World Journal of Engineering and Technology, 2014, pp.92-99
- 31. Paul Du Bois, Clifford C. Chou et al.:** ‘ Vehicle Crashworthiness and occupant Protection’, American Iron and Steel Institute, 2004
- 32. Jacob G.C., Fellers J.F., Simunovic S. et al.:** ‘Energy Absorption in Polymer Composites for automotive crashworthiness’, Journal of composite materials, 2002.
- 33. George C. Jacob, John F. Fellers et al.:** ‘ Crashworthiness of Automotive Composite Material Systems’, Journal of Applied Polymer Science, Vol. 92, 2004, pp. 3218-3225.

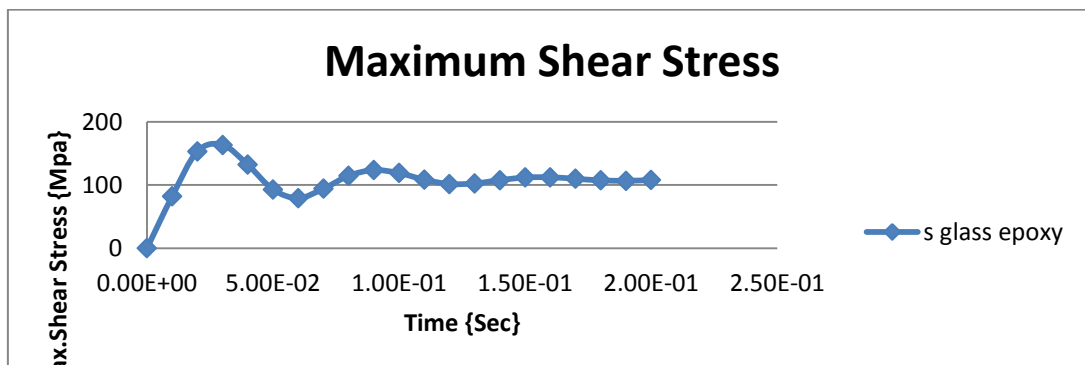
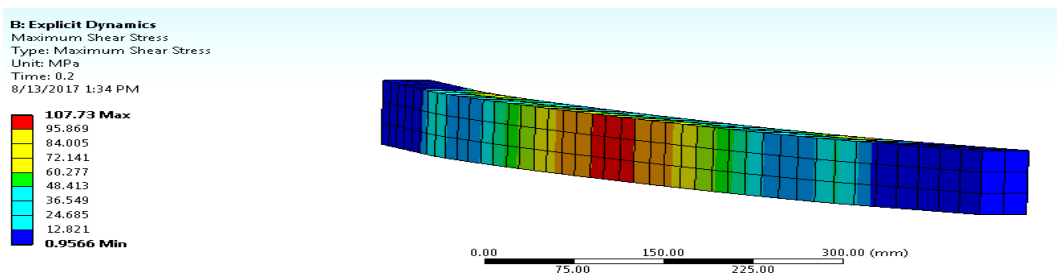
- 34. C.Lopes, Z.Giirdal, P.P.Camanho et al.:** 'Simulation of low-velocity impact damage on composite laminates', 50th AIAA/ASME/ASCE/AHS/ASC structures, structural dynamics, and materials conference, California, May 2009.
- 35. Serge Abrate:** 'Impact engineering of composite structures', CISM courses and lectures
- 36. George C. Jacob, John F. Fellers et al.:** 'Crashworthiness of Automotive Composite Material Systems', Journal of Applied Polymer Science, Vol. 92, 2004, pp. 3218-3225.
- 37. Zhang Jingwen, et al.,** "Light weight replacement and the optimization design of bumper beam based on crash safety", engineering.cae.cn, Vol. 12 No. 5, 2014
- 38. www.azom.com.**

APPENDIX A

Maximum shear stress of a conventional steel bumper beam



Maximum shear stress developed in a composite beam



APPENDIX B

Properties of Composite

The property of composite can be estimated numerically by combining the fiber (f) and matrix (m) properties. V is volume fraction, [25].

1. Lamina Density,

$$\rho_c = \rho_f V_f + \rho_m V_m$$

2. Longitudinal Young's Modulus,

$$E_1 = E_f V_f + E_m V_m$$

3. Transverse Young's Modulus

$$\frac{1}{E_2} = \frac{V_m}{E_m} + \frac{V_f}{E_f}$$

4. In-Plane Poisson's Ratio,

$$\nu_{12} = \nu_f V_f + \nu_m V_m$$

5. In-Plane Shear Modulus

$$G_{12} = G_m \left[\frac{(1 + V_f) + (1 - V_f) \frac{G_m}{G_f}}{(1 - V_f) + (1 + V_f) \frac{G_m}{G_f}} \right]$$

